SCIENCE CHINA
Information Sciences

• RESEARCH PAPER •

September 2026, Vol. 69, Iss. 9, 192208:1–192208:18
https://doi.org/10.1007/s11432-026-5079-x

Asymptotical event-based boundary fault-tolerant control for cascaded ODE-belt systems with prescribed-time performance

Yukan ZHENG[1,4], Xiangqian YAO[2], Yu LIU[1,3*] & Ju H. PARK[4*]

[1]*School of Automation Science and Engineering, South China University of Technology, Guangzhou 510640, China*
[2]*School of Future Technology, South China University of Technology, Guangzhou 510640, China*
[3]*Engineering Research Center of Precision Electronic Manufacturing Equipment, Ministry of Education, Guangzhou 510640, China*
[4]*Department of Electrical Engineering, Yeungnam University, Gyeongsan 38541, Republic of Korea*

Received 28 January 2026/Revised 7 May 2026/Accepted 15 June 2026/Published online 1 September 2026

Abstract This paper focuses on event-based boundary fault-tolerant control for deferred-constrained cascaded ordinary differential equation (ODE)-belt systems modeled by flexible axially moving belt and nonlinear actuator dynamics subject to unknown parameters, nonlinearities, and actuator failure. To reduce the continuous updating of input signal, a dynamic threshold triggering mechanism is developed. Under these multiple constraints, achieving the asymptotic convergence of cascaded systems presents significant challenges for control design. In control design, radial basis neural networks are used to approximate uncertain nonlinear functions. The prescribed performance funnel and adaptive backstepping technique are applied to skillfully achieve the prescribed performance. Based on the designed adaptive failure compensator, the effect of actuator fault can be compensated for completely. Based on the Barrier Lyapunov function (BLF) approach, a novel boundary event-based fault-tolerant control protocol is successfully designed to achieve asymptotic convergence and vibration suppression. Remarkably, the appealing feature of the designed controller lies in the smooth function norm with a positive integrable function, which makes the controller powerful enough to achieve asymptotic convergence. Furthermore, the Zeno behavior can be excluded. Lastly, some simulation results are presented to validate the constructed results.

Keywords flexible axially moving system, actuator dynamics, asymptotical control, event-based fault-tolerant control, prescribed-time performance

Citation Zheng Y K, Yao X Q, Liu Y, et al. Asymptotical event-based boundary fault-tolerant control for cascaded ODE-belt systems with prescribed-time performance. Sci China Inf Sci, 2026, 69(9): 192208, https://doi.org/10.1007/s11432-026-5079-x

1 Introduction

Boundary control of axially moving systems has drawn much interest in recent decades due to its numerous practical applications, such as axially moving strings, flexible manipulators, and axially moving belt [1–7]. The characteristics of the axially moving systems result in elastic vibration during operation, thereby diminishing work efficiency, reducing service life, and posing safety hazards. The axially moving belt system of surface mount technology (SMT) equipment is often characterized by high acceleration/deceleration, which is often characterized as partial differential equations (PDEs) due to their infinite-dimensional characteristics.

Although remarkable results have been proposed for axially moving systems, there remain problems to be resolved, particularly regarding the actuator dynamics at the boundary. Such systems are generally referred to as cascaded PDE-ODE systems since the actuator dynamics are typically modeled by ordinary differential equations (ODEs). On the boundary control of cascaded systems, some preliminary results have been obtained for the reaction-diffusion equation [8, 9] and Burgers' equation [10] with first-order linear actuator dynamics but are restricted to the simple form of actuator dynamics. Meanwhile, vibration control of flexible structures with first-order actuator dynamics was explored, as in flexible wings [11], hypersonic vehicles [12], and axially moving systems [13, 14]. Remarkably, these methods are only applicable to linear actuator dynamics without uncertainty and nonlinearity and cannot be directly implemented for axially moving systems with uncertain actuator dynamics. Boundary control problems for parabolic/hyperbolic equations with uncertain high-order actuator dynamics were investigated [15, 16] using the infinite/finite-dimensional backstepping method, but neglecting the complicated flexible PDE models.

* Corresponding author (email: auylau@scut.edu.cn, jessie@ynu.ac.kr)

In practical systems, it is noteworthy that constraint problems inevitably exist in various applications due to security criteria, performance requirements, and physical limitations. Numerous researchers have been devoted to constraint control of nonlinear systems, e.g., constant constraint, time-varying constraint, and prescribed performance control (PPC) [17–19], but the tracking error only converges to a small region whose size depends on the design parameters and initial conditions, meaning that the tracking accuracy cannot be predetermined. Recently, several well-known research results on prescribed-time performance control (PTPC) [20, 21] have been presented to handle this issue. For example, the input-constrained PTPC for nonlinear systems was designed [20]. Unknown actuator failures may lead to performance degradation and, in severe cases, destructive accidents [22]. The prescribed performance fault-tolerant control (PPFTC) of nonlinear systems and MIMO uncertain systems was studied [23, 24]. The sensor fault compensation for parametric strict-feedback systems was explored [25] based on the proposed output-feedback failure compensator. The actuator fault compensation problem and unknown control direction for nonlinear systems subject to unknown control directions was addressed [26, 27] by using the Nussbaum function method. Recently, considering the coupling systems, some adaptive FTC schemes have been proposed for cascaded ODE-string/beam and string-beam systems [13, 14, 28]. However, owing to the coexistence of uncertain high-order actuator dynamics and actuator failures, the existing approaches for boundary control cannot be extended directly to boundary fault-tolerant control for constrained cascaded ODE-belt systems.

Recently, event-triggered control (ETC) has been developed to reduce the communication burden and save the communication resources [29–32]. For example, the finite-time asymptotic event-triggered control for nonlinear multi-agent systems was proposed [33] utilizing the adaptive radial basis function neural network (RBFNN). The output-feedback boundary event-based control was proposed [34], while the observer-based asymptotic event-triggered control for hyperbolic PDE-ODE systems was designed [35]. Boundary event-triggered control for a flexible beam was explored [36] through the BLF method, where only bounded stabilization error was realized. Fully distributed dynamic event-triggered containment control for linear multi-agent systems subject to multiple types of disturbances was researched in [37], in which only uniformly ultimately bounded (UUB) stability can be achieved. However, it is pointed out that the tracking/stabilization errors [29, 30, 36, 37] only converge to the neighborhood of zero. Thus, for asymptotical dynamic event-based control of cascaded ODE-belt systems involving actuator failures, unknown parameters, and deferred constraints, more techniques should be further developed.

Motivated by the preceding discussion, this paper investigates an adaptive event-based boundary control problem for cascaded ODE-belt systems subject to unknown parameters, uncertainties, prescribed-time performance, and actuator failures. Under these constraints, we organically use the boundary control, backstepping control, prescribed performance funnel, and event-based control in control design to realize the asymptotic convergence for cascaded ODE-belt systems. This strategy faces the following technical challenges. In contrast to existing results [1–7] where flexible structures are free of actuator dynamics, this paper concentrates primarily on a flexible axially moving belt with uncertain nonlinear actuator dynamics. While some excellent boundary algorithms have been presented [8–14], they are restricted to systems without nonlinearities and uncertainties, and thus they cannot be directly applicable to achieve vibration suppression of cascaded ODE-belt with uncertainties and nonlinearities. Due to the presence of actuator dynamics, particularly the uncertainties or nonlinearities therein, certain essential obstacles emerge in control design and performance analysis, making the control problem much more challenging. Thus, it is meaningful and challenging to explore the boundary control for cascaded ODE-belt systems. Though some excellent ETC schemes have been obtained for PDEs [34–37], they are limited to systems without actuator dynamics, and these approaches cannot be directly applied to the axially moving belt with high-order actuator dynamics. In this paper, the switching threshold triggering strategy is further developed for cascaded ODE-belt systems.

In general, the main contributions are summarized as follows.

(i) Compared to the existing results in [8–14], where the actuator dynamics is limited to first-order linear actuator dynamics, this paper further explores a more general type of actuator dynamics with uncertainties and nonlinearities. Moreover, the effects of actuator failures can be adaptively compensated by the fault-tolerant controller, which contains an adaptive failure compensation coefficient. The asymptotical vibration suppression of cascaded ODE-belt systems can be achieved despite the effects of actuator failure, uncertainties, and nonlinearities, in contrast to the UUB results in [1–6].

(ii) By introducing a special kind of prescribed-time performance funnel, together with the BLF method and backstepping method, a novel boundary adaptive control scheme is proposed that governs the error variables to evolve within the prescribed boundary region after a preset finite time. The settling time can be explicitly set independent of the initial conditions and design parameters. The transient performance and static performance can be ensured through the designed boundary funnel control.

(iii) Unlike [34–37], a new dynamic threshold triggering strategy is proposed for the cascaded ODE-belt systems.

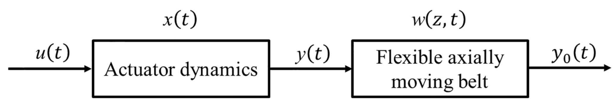

Figure 1 Cascade of axially moving belt system with actuator dynamics.

By introducing the smooth functions with respect to positive integrable functions, the developed event-based control can achieve zero stabilization error. A new control framework is developed for the boundary control of cascaded systems.

This paper has been structured as follows. Section 2 illustrates the cascaded systems model, control objective, and some preliminaries. The prescribed-time performance funnel, event-based fault-tolerant control design, and stability analysis are presented in Section 3. The simulation and conclusion are shown in Sections 4 and 5.

2 Problem statements and preliminaries

Remark 1. Let $(\cdot)(z,t)=(\cdot)(z)$, $(\cdot)(L,t)=(\cdot)(L)$, $\forall z\in[0,L], t\in[0,\infty)$, $(\cdot)(0,t)=(\cdot)(0)$, $\partial(\cdot)/\partial z=(\cdot)_z$, and $\partial(\cdot)/\partial t=(\cdot)_t$.

Consider the cascaded system models consisting of a flexible axially moving belt [3] and uncertain nonlinear actuator dynamics shown in Figure 1, modeled by

$$\begin{aligned}&mw_{tt}(z)+ma(t)w_z(z)+2m\nu(t)w_{zt}(z)-Tw_{zz}(z)\\&\quad+m\nu^2(t)w_{zz}(z)+cw_t(z)+c\nu(t)w_z(z)=0, &\text{(1a)}\\&m_cw_{tt}(L)+Tw_z(L)+d_sw_t(L)=y(t), &\text{(1b)}\\&w(0)=0, &\text{(1c)}\\&y_0(t)=C_0\left[w(L,t),w_t(L,t),w_z(L,t)\right]^\top, &\text{(1d)}\\&\dot{x}_i(t)=x_{i+1}(t)+\varphi_i^\top(\bar{x}_i)\theta+f_i(\bar{x}_i), &\text{(1e)}\\&\dot{x}_n(t)=u(t)+\varphi_n^\top(x)\theta+f_n(x), &\text{(1f)}\\&y(t)=x_1(t), &\text{(1g)}\end{aligned}$$

where $i=1,\ldots,n-1$, $w(z,t)$ $((z,t)\in(0,L)\times[0,+\infty))$ is the vibration displacement, L and T are the length and tension of the belt. $\nu(t)$ and $a(t)$ denote the axial speed and acceleration of the belt (see Figure 1 in [3]), respectively. m_c denotes the actuator's mass, m denotes the mass per unit length, d_s and c are the damping coefficient of the actuator and viscous, $y_0(t)\in\mathbb{R}^q$ denotes the measurement of the belt at the boundary including the velocity, or their combinations at the free end of the belt, and $C_0\in\mathbb{R}^{q\times 2}$ is a known matrix. x_i represents the actuator state with $\bar{x}_i=(x_1,\ldots,x_i)^\top\in\mathbb{R}^i$ and $x=\bar{x}_n$, $u(t)$ and $y(t)$ denote the control input and output of the actuator dynamics, $\theta\in\mathbb{R}^r$ is the unknown parameter vector, $\varphi_i(\cdot):\mathbb{R}^i\to\mathbb{R}^r$ is the smooth nonlinear function, $f_i(\bar{x}_i)$ is the unknown continuous function.

Most of the existing studies merely consider the actuation of axially moving system boundaries, regardless of the actuator dynamics. In many practical applications, due to the increased process demands, the actuator dynamics characteristics cannot be neglected but should be jointly considered with the controlled plant. Additionally, $w(L)$ and $w_z(L)$ can be measured by the laser displacement sensor and the boundary inclinometer, $w_t(L)$ is calculated utilizing the backward difference method, and $x_i(t)$ can be measured by relevant sensors.

Define $u_f(t)$ as the input signal of the controller $u(t)$. The types of failures can be modeled as follows [22, 23]:

$$u(t)=\rho u_f(t)+u_s,\forall t\geqslant t_f,\ \rho u_s=0, \tag{2}$$

where $\rho\in[0,1)$ and u_s denote the stuck failure. Eq. (2) indicates that the actuator fails suddenly from t_f and implies the following three cases. (1) $\rho=1$ and $u_s=0$, the failure-free case; (2) $0<\underline{\rho}<\rho<1$ and $u_s=0$, the partial loss of effectiveness (PLOE); and (3) $\rho=0$ and $u_s\neq 0$. In case (3), u_s can no longer be influenced by the input signal u_f. This implies the total loss of effectiveness (TLOE).

In this paper, the following coordinate transformations are defined

$$e_1=w(L)=(x_1-m_cw_{tt}(L)-Tw_z(L))/d_s, \tag{3}$$
$$e_i=x_i-\alpha_{i-1},\ i=2,\ldots,n, \tag{4}$$

where $\alpha_1, \ldots, \alpha_{n-1}$ denote the virtual controllers to be determined later. To constrain the transient performance, the states are required to remain within the following constraints:

$$\Pi_{\zeta_i} := \{(t, e_i) \in \mathbb{R}_{\geqslant 0} \times \mathbb{R} | \ |e_i(t)| \leqslant \varepsilon_i\}. \tag{5}$$

For cascaded ODE-belt systems (1a)–(1g) with actuator failure (2), we aim to develop a boundary event-based adaptive failure compensation control protocol such that (i) closed-loop systems are uniformly bounded; (ii) e_i converge to the region $\{e_i||e_i| \leqslant \varepsilon_i, \forall t \geqslant T_{pi}\}$ with ε_i being the prescribed precision and T_{pi} being the prescribed settling time; (iii) asymptotical vibration suppression can be obtained, i.e., $\lim_{t\to\infty} |w(z,t)| = 0$; (iv) the Zeno behavior does not occur.

Remark 2. The cascaded ODE-belt systems under investigation have some distinctive characteristics. (1) The actuator dynamics is uncertain and nonlinear rather than the linear ones without any uncertainty [8–14]; (2) control input occurs in the actuator dynamics rather than in the PDE subsystem [1–7]; (3) the PDE subsystem is the axially moving belt which is more complex than the parabolic/hyperbolic equation [15, 16]. Hence, the existing control protocols are incapable of the vibration suppression of (1a)–(1g).

The following assumptions and lemmas play an essential role in the stability analysis of this paper.

Assumption 1 ([1]). There exist $b_i > 0$ $(i = 1, 2)$ such that $0 < \nu(t) \leqslant b_1$ and $|a(t)| \leqslant b_2$ since ν and a have finite energy and are uniformly continuous.

Assumption 2 ([22]). There exist positive values $\underline{\rho}$ and ϖ such that $\rho \geqslant \underline{\rho}$ and $|u_s| \leqslant \varpi$.

Assumption 3 ([38]). If the kinetic energy and potential energy of the belt are bounded, then $w_t(L)$, $w_{zt}(L)$, $w_z(L)$, and $w_{zz}(L)$ are said to be bounded.

Remark 3. Note that the boundedness assumption, i.e., Assumption 3, is obtained just from an engineering point of view. From [38], we also note that experimental results for real physical systems seem to prove that the engineer-based assumption is indeed true. Yet, from a strict mathematical point of view, one might question these boundedness assumptions since we cannot prove Assumption 3 by strict mathematical proof. Reviewing previous boundary control results, it seems that there is no well-established methodology for checking the boundedness of signals for nonlinear distributed parameter systems. A similar remark is also presented in [38].

Lemma 1 ([7]). For any $w_1(z,t)$, $w_2(z,t)$ with $(z,t) \in [0, L] \times [0, +\infty)$ and $\psi > 0$, there hold

$$\begin{cases} w_1 w_2 \leqslant |w_1 w_2| \leqslant w_1^2 + w_2^2, \\ |w_1 w_2| = |(\frac{1}{\sqrt{\psi}} w_1)(\sqrt{\psi} w_2)| \leqslant \frac{1}{\psi} w_1^2 + \psi w_2^2. \end{cases} \tag{6}$$

Lemma 2 ([7]). $w(z,t)$ $((z,t) \in [0, L] \times [0, +\infty))$ is a function with $w(0,t) = 0$. Then there hold

$$\begin{cases} \int_0^L w^2 dz \leqslant L^2 \int_0^L w_z^2 dz, \\ w^2 \leqslant L \int_0^L w_z^2 dz. \end{cases} \tag{7}$$

Lemma 3 ([33]). For unknown continuous function $\mathcal{F}(\mathcal{X}) : \Omega_{\mathcal{X}} \to \mathbb{R}$ defined on $\Omega_{\mathcal{X}} \subseteq \mathbb{R}^q$, there exist an RNFNN such that $\mathcal{F}(\mathcal{X}) = \mathcal{W}^{*\top} \mathcal{S}(\mathcal{X}) + \hbar(\mathcal{X}), \hbar(\mathcal{X}) \leqslant \bar{\hbar}$ in which $\mathcal{W}^* = [\mathcal{W}_1^*, \ldots, \mathcal{W}_p^*]^\top \in \mathbb{R}^p$ represents the optimal weight matrix, $\mathcal{X} = [\mathcal{X}_1, \ldots, \mathcal{X}_q]^\top \in \Omega_{\mathcal{X}}$ denotes the input vector, $\mathcal{S}(\mathcal{X}) = [\mathcal{S}_1(\mathcal{X}), \ldots, \mathcal{S}_p(\mathcal{X})]^\top \in \mathbb{R}^p$ denotes the basis function. $\mathcal{S}_i(\mathcal{X})$ $(i = 1, \ldots, p)$ is generally selected as a Gaussian function $\mathcal{S}_i(\mathcal{X}) = e^{-(\mathcal{X} - C_i)^\top (\mathcal{X} - C_i)/a_i^2}$, where a_i is the width and $C_i \in \mathbb{R}^q$ is the center of the receptive field.

3 Main results

In this section, a new control design framework to solve boundary control problem for cascaded ODE-belt systems is presented. Firstly, we introduce the prescribed-time performance funnel to incorporate the desired transient performance metrics. Then, an adaptive event-based boundary fault-tolerant control protocol is designed by integrating the bounded estimation method and BLF-based backstepping design. The block diagram of the boundary control scheme is shown in Figure 2.

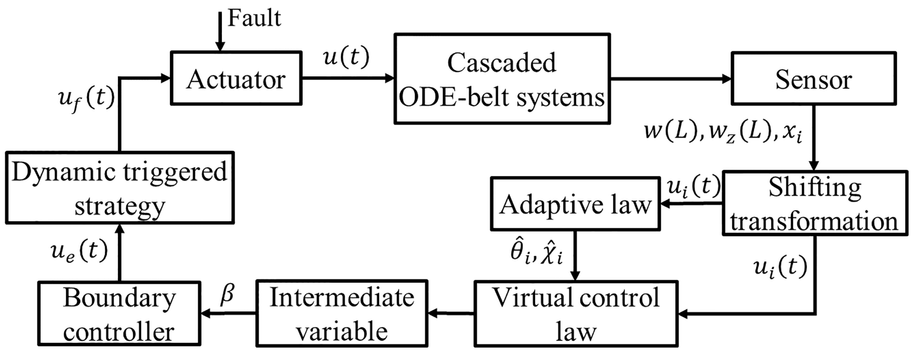

Figure 2 Block diagram of the boundary control strategy.

3.1 Prescribed-time performance funnel

To achieve the desired transient performance and constraint performance, the following prescribed-time performance funnel function is inspired by [20].

Definition 1. For given accuracy $\varepsilon > 0$ and convergence settling time T_p, a time-varying function $\zeta(\varepsilon, T_p, t), t \geqslant 0$ is said to be a prescribed-time performance function, when

(1) $\zeta(t) > 0$ for $t > 0$ and $\zeta(0) = 0$;

(2) $\zeta(t) \in \mathcal{W}^{1,\infty}$ where $\mathcal{W}^{1,\infty}$ is a class of bounded functions with bounded derivatives;

(3) for any $t_\varepsilon < T_p$, there holds $\zeta(t) \geqslant 1/\varepsilon$ for $t > t_\varepsilon$.

Then, on the basis of $\zeta(t)$, the performance funnel is defined as follows:

$$\Pi_\zeta : = \{(t, e) \in \mathbb{R}_{\geqslant 0} \times \mathbb{R} |\ |e(t)|\zeta(t) < 1\}. \tag{8}$$

In this paper, to constrain the transient performance, the performance funnel is defined as

$$\Pi_{\zeta_i} : = \{(t, e_i) \in \mathbb{R}_{\geqslant 0} \times \mathbb{R} |\ |e_i(t)| \leqslant \varepsilon_i\}. \tag{9}$$

Remark 4. Unlike the existing results, $\zeta_i(t)$ has the following advantages: (1) the funnel boundary decided by $\zeta_i(t)$ enforces a transient behavior boundary on variable e_i; (2) $e_i(0)\zeta_i(0) < 1$ hold since $\zeta_i(0) = 0$, and hence the restriction on the initial conditions is removed; (3) the settling time T_{pi} and convergence accuracy ε_i can be predetermined and the performance bound can reflect the control objective (the predetermined accuracy within the preset finite time) and independent of the design parameters and initial conditions.

By constructing a feasible control law to ensure vibration deflection $w(L)$ and actuator state x_i always evolve within the funnel Π_{ζ_i}, the desired transient performance specifications can be obtained.

There are many choices for $\zeta_i(t)$, such as

$$\zeta_i(t) = \begin{cases} \frac{1}{\varepsilon_i}(1 - (\frac{T_{pi} - t}{T_{pi}})^{q_i}), & 0 \leqslant t \leqslant T_{pi}, \\ \frac{1}{\varepsilon_i}, & t > T_{pi}, \end{cases} \tag{10}$$

and $\zeta_i(t) = \frac{t}{\varepsilon_i[(1-\varrho_i)t + \varrho_i T_{pi}]}$ with $q_i \geqslant 2,\ \varrho_i \in (0, 1)$ being positive values.

3.2 Adaptive event-based boundary fault-tolerant control design

This subsection aims to develop an adaptive FTC to guarantee that $e_i(t)$ converges within the predefined funnel.

Firstly, design the Lyapunov function candidate

$$\mathcal{V}_L = \mathcal{V}_1 + \mathcal{V}_2, \tag{11}$$

$$\mathcal{V}_1 = \frac{\gamma m}{2} \int_0^L (w_t + \nu w_z)^2 dz + \frac{\gamma T}{2} \int_0^L w_z^2 dz, \tag{12}$$

$$\mathcal{V}_2 = 2\lambda m \int_0^L z w_z (w_t + \nu w_z) dz \tag{13}$$

with γ, λ being positive values.

Lemma 4. The Lyapunov function (11) satisfies the following property:

$$0 \leqslant \sigma_2 \mathcal{V}_1 \leqslant \mathcal{V}_L \leqslant \sigma_3 \mathcal{V}_1 \tag{14}$$

with $\sigma_2 = 1-\sigma$ and $\sigma_3 = 1+\sigma$.

Proof. It follows from Young's inequality and Poincaré's inequality that

$$|\mathcal{V}_2| \leqslant \lambda m L \left(\int_0^L (w_t + \nu w_z)^2 dz + \int_0^L w_z^2 dz \right) \leqslant \sigma \mathcal{V}_1 \tag{15}$$

with $\sigma = [(2\lambda m L)/\min(\gamma T, \gamma m)]$, and hence, $-\sigma\mathcal{V}_1 \leqslant \mathcal{V}_2 \leqslant \sigma \mathcal{V}_1$. Further, it is easy to get

$$0 < (1-\sigma)\mathcal{V}_1 \leqslant \mathcal{V}_L \leqslant (1+\sigma)\mathcal{V}_1. \tag{16}$$

Assuming $0<\sigma<1$ and $\lambda < [\min(\gamma T, \gamma m)/(2mL)]$, there holds $\sigma_2\mathcal{V}_1 \leqslant \mathcal{V}_L \leqslant \sigma_3 \mathcal{V}_1$.

Next, we can obtain that $\dot{\mathcal{V}}_1 = F_1 + \mathcal{F}_2 + \mathcal{F}_3 + \mathcal{F}_4$ with $\mathcal{F}_1 = \gamma m \int_0^L (a w_t w_z + a\nu w_z^2) dz$, $\mathcal{F}_2 = \gamma m \int_0^L (w_t w_{tt} + \nu w_z w_{tt}) dz$, $\mathcal{F}_3 = \gamma m \int_0^L (\nu w_t w_{zt} + \nu^2 w_z w_{zt}) dz$, and $\mathcal{F}_4 = \gamma T \int_0^L w_z w_{zt} dz$.

Substituting (1a) to $\mathcal{F}_2$, using integration by parts, it can be obtained that

$$\begin{aligned} \mathcal{F}_2 =& \frac{\gamma\nu(T-m\nu^2)}{2} w_z^2(L) - \gamma m \nu w_t^2(L) - \gamma m \nu a \int_0^L w_z^2 dz - 2\gamma m \nu^2 w_z(L) w_t(L) \\ & - \gamma c \int_0^L (w_t+\nu w_z)^2 dz - \left(\frac{\gamma \nu T}{2} - \frac{\gamma m \nu^3}{2}\right) w_z^2(0) + \gamma(T+m\nu^2) \int_0^L w_t w_{zz} dz \\ & - \gamma m a \int_0^L w_t w_z dz. \end{aligned} \tag{17}$$

Integrating $\mathcal{F}_3$ and $\mathcal{F}_4$ by parts, one has

$$\mathcal{F}_3 = \gamma m \nu^2 w_z(L) w_t(L) + \frac{\gamma m \nu}{2} w_t^2(L) - \gamma m \int_0^L \nu^2 w_t w_{zz} dz, \tag{18}$$

$$\mathcal{F}_4 = \gamma T w_t(L) w_z(L) - \gamma T \int_0^L w_t w_{zz} dz. \tag{19}$$

Based on the above inequalities, the derivative of $\mathcal{V}_1$ can be obtained as

$$\begin{aligned} \dot{\mathcal{V}}_1 \leqslant & -\gamma c \int_0^L (w_t+\nu w_z)^2 dz - \frac{\gamma\nu(T-m\nu^2)}{2} w_z^2(0) + \left(\frac{\gamma\nu T}{2} - \frac{\gamma T \delta_1}{2}\right) w_z^2(L) \\ & - \frac{\gamma T}{2\delta_1} w_t^2(L) + \frac{\gamma T}{2\delta_1} [w_t(L) + \delta_1 w_z(L)]^2 - \frac{\gamma m \nu}{2} [w_t(L) + \nu w_z(L)]^2, \end{aligned} \tag{20}$$

where δ_1 is a positive parameter.

Similarly, it can be derived that $\dot{\mathcal{V}}_2 = \mathcal{J}_1 + \mathcal{J}_2$ with $\mathcal{J}_1 = 2\lambda m \int_0^L z w_z (w_{tt} + a w_z + \nu w_{zt}) dz$ and $\mathcal{J}_2 = 2\lambda m \int_0^L z w_{zt} (w_t + \nu w_z) dz$. By using integration by parts, it yields that

$$\begin{aligned} \mathcal{J}_1 =& \lambda T L w_z^2(L) - \lambda m L \nu^2 w_z^2(L) - 2\lambda c \nu \int_0^L z w_z^2 dz + \lambda m \int_0^L \nu^2 w_z^2 dz \\ & - 2\lambda c \int_0^L z w_z w_t dz - \lambda T \int_0^L w_z^2 dz - 2\lambda m \nu \int_0^L z w_z w_{zt} dz, \end{aligned} \tag{21}$$

$$\mathcal{J}_2 = 2\lambda m \nu \int_0^L z w_t w_{zt} dz - \lambda m \int_0^L w_t^2 dz + \lambda m L w_t^2(L). \tag{22}$$

Hence, a combination of Lemmas 1 and 2 yields that

$$\begin{aligned} \dot{\mathcal{V}}_2 \leqslant & -(\lambda T - \lambda m b_1^2 - 2\lambda c L \delta_2) \int_0^L w_z^2 dz - \lambda m \int_0^L w_t^2 dz \\ & + \frac{2\lambda c L}{\delta_2} \int_0^L (w_t + \nu w_z^2) dz - \lambda L (m\nu^2 - T) w_z^2(L) + \lambda m L w_t^2(L), \end{aligned} \tag{23}$$

where δ_2 is a positive value.

By integrating the above results, we can obtain

$$\begin{aligned}\dot{\mathcal{V}}_L \leqslant &-\tau_1\int_0^L w_t^2dz-\tau_2\int_0^L w_z^2dz-\tau_3\int_0^L(w_t+\nu w_z)^2dz\\&-\tau_4w_z^2(0)-\tau_5w_z^2(L)-\tau_6w_t^2(L)+\frac{\gamma T}{2\delta_1}[w_t(L)+\delta_1w_z(L)]^2,\end{aligned}\tag{24}$$

where $\tau_1=\lambda m$, $\tau_2=\lambda T-\lambda mb_1^2-2\lambda cL\delta_2$, $\tau_3=\gamma c-\frac{2\lambda cL}{\delta_2}$, $\tau_4=\frac{\gamma T\nu-\gamma m\nu^3}{2}$, $\tau_5=\lambda mL\nu^2-\frac{\gamma T\nu}{2}+\frac{\gamma T\delta_1}{2}-\lambda TL$, and $\tau_6=\frac{\gamma T}{2\delta_1}-\lambda mL$.

To ensure $e_i(t)$ remains within the predefined funnel, we define the following shifting transformation to carry out constraint control

$$u_i=\zeta_i(t)e_i,\ \ i=1,2,\ldots,n\tag{25}$$

with $\zeta_i(t)$ being the prescribed-time performance function defined in Definition 1.

Step 1: Using (1a)–(1g) and (3), the derivative of e_1 can be reduced to

$$\dot{e}_1=(e_2+\alpha_1+\varphi_1^\top\theta+\Phi+f_1)/d_s\tag{26}$$

with $\Phi=-m_cw_{tt}(L)-Tw_z(L)$, and then $\dot{u}_1=\dot{\zeta}_1e_1+\zeta_1(e_2+\alpha_1+\varphi_1^\top\theta+\Phi+f_1)/d_s$.

Choose the Barrier Lyapunov function candidate

$$\mathcal{V}_{L1}=\mathcal{V}_L+\frac{1}{2}\log\frac{1}{1-u_1^2}+\frac{1}{2\gamma_{11}}\tilde{\theta}_1^\top\tilde{\theta}_1+\frac{1}{2\gamma_{12}}\tilde{\chi}_1^2,\tag{27}$$

where $\tilde{\theta}_1=\theta-\hat{\theta}_1$, $\tilde{\chi}_1=\chi_1-\hat{\chi}_1$, and γ_{11},γ_{12} are positive scalars. Note that $\mathcal{V}_{L1}$ is positive definite and continuously differentiable for $|u_1|<1$, and so is $\mathcal{V}_{Li}$ for $|u_i|<1$.

Using (24), we have

$$\begin{aligned}\dot{\mathcal{V}}_{L1}\leqslant &-\tau_1\int_0^L w_t^2dz-\tau_2\int_0^L w_z^2dz-\tau_3\int_0^L(w_t+\nu w_z)^2dz-\tau_4w_z^2(0)\\&-\tau_5w_z^2(L)-\tau_6w_t^2(L)+\xi_1\dot{\zeta}_1u_1e_1+\frac{\gamma T}{2\delta_1}[w_t(L)+\delta_1w_z(L)]^2\\&+\frac{\xi_1\zeta_1u_1}{d_s}(e_2+\alpha_1+\varphi_1^\top\theta+\Psi_1)-\frac{1}{\gamma_{11}}\tilde{\theta}_1^\top\dot{\hat{\theta}}_1-\frac{1}{\gamma_{12}}\tilde{\chi}_1\dot{\hat{\chi}}_1,\end{aligned}\tag{28}$$

where $\xi_1=\frac{1}{1-u_1^2}>0$ and $\Psi_1=f_1+\Phi$. Using Lemma 3, the uncertainty Ψ_1 can be determined by RBFNN, i.e., $\Psi_1=\mathcal{W}_1^{*\top}\mathcal{S}_1(\mathcal{X}_1)+\hbar_1(\mathcal{X}_1)$ with $\mathcal{X}_1=[x_1,w_z(L),w_t(L)]^\top$.

Defining $\chi_1=\sup_{t\geqslant0}\|\Theta_1(t)\|$ with $\Theta_1(t)=[\mathcal{W}_1^{*\top},\hbar_1]^\top$ and $\psi_1=[\mathcal{S}_1(\mathcal{X}_1),1]^\top$, and invoking inequality $|\pi|-\frac{\pi^2}{\sqrt{\pi^2+\varrho^2}}\leqslant\varrho$ with $\pi\in\mathbb{R}$ and $\varrho>0$ [33], there holds

$$\begin{aligned}\frac{1}{d_s}\xi_1\zeta_1u_1(\mathcal{W}_1^{*\top}\mathcal{S}_1+\hbar_1)&=\frac{1}{d_s}\xi_1\zeta_1u_1\Theta_1^\top\psi_1\\&\leqslant\frac{1}{d_s}\xi_1\zeta_1|u_1|\chi_1\psi_1\leqslant\frac{1}{d_s}\chi_1\kappa_1+\frac{1}{d_s}\xi_1\zeta_1u_1\eta_1\chi_1,\end{aligned}\tag{29}$$

where $\eta_1=[(\xi_1\zeta_1u_1\psi_1^\top\psi_1)(\sqrt{\xi_1^2\zeta_1^2u_1^2\psi_1^\top\psi_1+\kappa_1^2})]$ and $\kappa_1>0$ is an integral function which satisfies $\int_0^t\kappa_1(t)dt\leqslant\bar{\kappa}_1$ with $\bar{\kappa}_1>0$ being a positive constant.

Choose the virtual control and adaptive updating laws

$$\alpha_1=-\frac{c_1u_1d_s}{\xi_1\zeta_1}-\frac{\dot{\zeta}_1e_1d_s}{\zeta_1}-d_s\hat{\theta}_1^\top\varphi_1-\frac{\hat{\chi}_1\eta_1}{d_s}-\frac{\gamma T[w_t(L)+\delta_1w_z(L)]^2}{2\delta_1(\xi_1u_1\zeta_1+\epsilon)},\tag{30}$$

$$\dot{\hat{\theta}}_1=\gamma_{11}\xi_1\zeta_1u_1\varphi_1/d_s-\gamma_{11}\kappa_1\hat{\theta}_1,\tag{31}$$

$$\dot{\hat{\chi}}_1=\gamma_{12}\xi_1\zeta_1u_1\eta/d_s-\gamma_{12}\kappa_1\hat{\chi}_1,\tag{32}$$

where $c_1 > 0$ denotes a positive value and $\epsilon > 0$ is a small value designed to exclude the appearance of the controller chattering phenomenon.

Using (30)–(32) and $\xi_1\zeta u_1 e_2 = \xi_1 u_1 u_2$, then Eq. (28) can be rewritten as

$$\dot{\mathcal{V}}_{L1} \leqslant -\ell(w) - c_1 u_1^2 + \frac{\xi_1 u_1 u_2}{d_s} + \kappa_1\left(\tilde{\theta}_1^\top \hat{\theta}_1 + \tilde{\chi}_1\hat{\chi}_1 + \frac{\chi_1}{d_s}\right) \tag{33}$$

with $\ell(w) = \tau_1\int_0^L w_t^2 dz + \kappa_2\int_0^L w_z^2 dz + \tau_3\int_0^L (w_t+\nu w_z)^2 dz + \tau_4 w_z^2(0) + \tau_5 w_z^2(L) + \tau_6 w_t^2(L)$.

Step 2: Select the Barrier Lyapunov function candidate

$$\mathcal{V}_{L2} = \mathcal{V}_{L1} + \frac{1}{2}\log\frac{1}{1-u_2^2} + \frac{1}{2\gamma_{21}}\tilde{\theta}_2^\top\tilde{\theta}_2 + \frac{1}{2\gamma_{22}}\tilde{\chi}_2^2 \tag{34}$$

with $\tilde{\theta}_2 = \theta - \hat{\theta}_2$, $\tilde{\chi}_2 = \chi_2 - \hat{\chi}_2$, and γ_{21}, γ_{22} being positive constants.

From (25), we can obtain

$$\dot{u}_2 = \dot{\zeta}_2 e_2 + \zeta_2(e_3 + \alpha_2 + \varphi_2^\top\theta + f_2 - \dot{\alpha}_1), \tag{35}$$

and thus,

$$\begin{aligned}\dot{\mathcal{V}}_{L2} \leqslant & -\ell(w) - c_1 u_1^2 + \frac{\xi_1 u_1 u_2}{d_s} + \kappa_1\left(\tilde{\theta}_1^\top\hat{\theta}_1 + \tilde{\chi}_1\hat{\chi}_1 + \frac{\chi_1}{d_s}\right) + \xi_2\dot{\zeta}_2 u_2 e_2 \\ & + \xi_2\zeta_2 u_2\left[e_3 + \alpha_2 - \Delta_2 + \Psi_2 + \left(\varphi_2^\top - \frac{\partial\alpha_1}{\partial x_1}\varphi_1^\top\right)\theta\right] - \frac{1}{\gamma_{21}}\tilde{\theta}_2^\top\dot{\hat{\theta}}_2 - \frac{1}{\gamma_{22}}\tilde{\chi}_2^\top\dot{\hat{\chi}}_2\end{aligned} \tag{36}$$

with $\xi_2 = \frac{1}{1-u_2^2}$, $\Delta_2 = \frac{\partial\alpha_1}{\partial x_1}x_2 + \frac{\partial\alpha_1}{\partial\hat{\chi}_1}\dot{\hat{\chi}}_1 + \frac{\partial\alpha_1}{\partial\hat{\theta}_1}\dot{\hat{\theta}}_1$, and $\Psi_2 = f_2 + \frac{\partial\alpha_1}{\partial x_1}f_2 + \frac{\partial\alpha_1}{\partial w_z(L)}w_{zt}(L) + \sum_{j=0}^{1}\frac{\partial\alpha_1}{\partial\zeta_1^{(j)}}\zeta_1^{(j+1)} + \frac{\partial\alpha_1}{\partial w_t(L)}w_{tt}(L)$. Using Lemma 3, we have $\Psi_2 = \mathcal{W}_2^{*\top}\mathcal{S}_2(\mathcal{X}_2) + \hbar_2$ with $\mathcal{X}_2 = [x_1, x_2, w_{zt}(L), w_{tt}(L), \zeta_1, \dot{\zeta}_1]^\top$.

Defining $\chi_2 = \sup_{t\geqslant 0}\|\Theta_2(t)\|$ with $\Theta_2(t) = [\mathcal{W}_2^{*\top}, \hbar_2]^\top$ and $\psi_2 = [\mathcal{S}_2, 1]^\top$, it can be derived that

$$\xi_2\zeta_2 u_2\Psi_2 \leqslant \chi_2\kappa_1 + \xi_2\zeta_2 u_2\eta_2\chi_2 \tag{37}$$

with $\eta_2 = [(\xi_2\zeta_2 u_2\psi_2^\top\psi_2)(\sqrt{\xi_2^2\zeta_2^2 u_2^2\psi_2^\top\psi_2 + \kappa_1^2})]$.

The virtual control and adaptive updating laws are designed as

$$\alpha_2 = -\frac{c_2 u_2}{\xi_2\zeta_2} - \frac{\xi_1\zeta_1 u_1}{\xi_2\zeta_2^2 d_s} - \frac{\dot{\zeta}_2 e_2}{\zeta_2} - \hat{\theta}_2^\top\left(\varphi_2 - \frac{\partial\alpha_1}{\partial x_1}\varphi_1\right) - \hat{\chi}_2\eta_2 + \Delta_2, \tag{38}$$

$$\dot{\hat{\theta}}_2 = \gamma_2\xi_2\zeta_2 u_2\left(\varphi_2 - \frac{\partial\alpha_1}{\partial x_1}\varphi_1\right) - \gamma_2\kappa_1\hat{\theta}_2, \tag{39}$$

$$\dot{\hat{\chi}}_2 = \gamma_{22}\xi_2\zeta_2 u_2\eta_2 - \gamma_{22}\kappa_1\hat{\chi}_2, \tag{40}$$

where c_2 is a positive value.

Substituting (38)–(40) into (36) yields that

$$\dot{\mathcal{V}}_{L2} \leqslant -\ell(w) - \sum_{s=1}^{2}(c_s u_s^2 + \kappa_1(\tilde{\theta}_s^\top\hat{\theta}_s + \tilde{\chi}_s\hat{\chi}_s)) + \kappa_1\left(\frac{\chi_1}{d_s} + \chi_2\right) + \xi_2 u_2 u_3. \tag{41}$$

Step i $(3 \leqslant i \leqslant n-1)$**:** Choose the Barrier Lyapunov function candidate

$$\mathcal{V}_{Li} = \mathcal{V}_{L(i-1)} + \frac{1}{2}\log\frac{1}{1-u_i^2} + \frac{1}{2\gamma_{i1}}\tilde{\theta}_i^\top\tilde{\theta}_i + \frac{1}{2\gamma_{i2}}\tilde{\chi}_i^2 \tag{42}$$

with $\tilde{\theta}_i = \theta - \hat{\theta}_i$, $\tilde{\chi}_i = \chi_i - \hat{\chi}_i$, and γ_{i1}, γ_{i2} being positive values.

From (25), we can obtain that

$$\dot{u}_i = \dot{\zeta}_i e_i + \zeta_i\left[e_{i+1} + \alpha_i + \left(\varphi_i^\top - \sum_{s=1}^{i-1}\frac{\alpha_{i-1}}{\partial x_s}\varphi_s^\top\right)\theta - \Delta_i + \Psi_i\right], \tag{43}$$

where $\Delta_i = \sum_{s=1}^{i-1} \frac{\partial \alpha_{i-1}}{\partial x_s} x_{s+1} + \sum_{s=1}^{i-1} \frac{\partial \alpha_{i-1}}{\partial \hat{\theta}_s} \dot{\hat{\theta}}_s + \sum_{s=1}^{i-1} \frac{\partial \alpha_{i-1}}{\partial \hat{\chi}_s} \dot{\hat{\chi}}_s$ and $\Psi_i = f_i + \sum_{s=1}^{i-1} \frac{\partial \alpha_{i-1}}{\partial x_s} f_s + \frac{\partial \alpha_{i-1}}{\partial w_t} w_{tt}(L) + \frac{\partial \alpha_{i-1}}{\partial w_z} w_{zt}(L) + \sum_{s=0}^{i-1} \sum_{j=0}^{1} \frac{\partial \alpha_{i-1}}{\partial \zeta_s^{(j)}} \zeta_s^{(j+1)}$.

Using (43), the derivative of $\mathcal{V}_{Li}$ yields

$$\begin{aligned} \dot{\mathcal{V}}_{Li} \leqslant & -\ell(w) - \sum_{s=1}^{i-1} [c_s u_s^2 + \kappa_1 (\tilde{\theta}_s^\top \hat{\theta}_s + \tilde{\chi}_s \hat{\chi}_s)] + \kappa_1 \left(\frac{\chi_1}{d_s} + \chi_2 \right) + \xi_i u_{i-1} u_i \\ & + \xi_i \dot{\zeta}_i u_i e_i + \xi_i \zeta_i u_i \left[e_{i+1} + \alpha_i - \Delta_i + \Psi_i + \left(\varphi_i^\top - \sum_{s=1}^{i-1} \frac{\partial \alpha_{i-1}}{\partial x_s} \varphi_s^\top \right) \theta \right] \\ & - \frac{1}{\gamma_{i1}} \tilde{\theta}_i^\top \dot{\hat{\theta}}_i - \frac{1}{\gamma_{i2}} \tilde{\chi}_i \dot{\hat{\chi}}_i \end{aligned} \tag{44}$$

with $\xi_i = \frac{1}{1-u_i^2}$. Defining $\chi_i = \sup_{t \geqslant 0} \|\Theta_i(t)\|$ with $\Theta_i(t) = [\mathcal{W}_i^{*\top}, \hbar_i]^\top$ and $\psi_i = [\mathcal{S}_i, 1]^\top$, we can get $\xi_i \zeta_i u_i \Psi_i \leqslant \chi_i \kappa_1 + \xi_i \zeta_i u_i \eta_i \chi_i$ with $\eta_i = [(\xi_i \zeta_i u_i \psi_i^\top \psi_i)(\sqrt{\xi_i^2 \zeta_i^2 u_i^2 \psi_i^\top \psi_i + \kappa_1^2})]$.

Select the virtual control and adaptive updating laws

$$\alpha_i = -\frac{c_i u_i}{\xi_i \zeta_i} - \frac{\xi_{i-1} u_{i-1}}{\xi_i \zeta_i} - \hat{\theta}_i^\top \left(\varphi_i - \sum_{s=1}^{i-1} \frac{\partial \alpha_{i-1}}{\partial x_s} \varphi_s \right) - \frac{\dot{\zeta}_i e_i}{\zeta_i} + \Delta_i - \hat{\chi}_i \eta_i, \tag{45}$$

$$\dot{\hat{\theta}}_i = \gamma_i \xi_i \zeta_i u_i \left(\varphi_i - \sum_{s=1}^{i-1} \frac{\partial \alpha_{i-1}}{\partial x_s} \varphi_s \right) - \gamma_i \kappa_1 \hat{\theta}_i, \tag{46}$$

$$\dot{\hat{\chi}}_i = \gamma_{i2} \xi_i \zeta_i u_i \eta_i - \gamma_{i2} \kappa_1 \hat{\chi}_i \tag{47}$$

with $c_i > 0$ being a value.

Substituting (45)–(47) into (44), it yields

$$\dot{\mathcal{V}}_{Li} \leqslant -\ell(w) - \sum_{s=1}^{i} [c_s u_s^2 + \kappa_1 (\tilde{\theta}_s^\top \hat{\theta}_s + \tilde{\chi}_s \hat{\chi}_s)] + \kappa_1 \left(\frac{\chi_1}{d_s} + \sum_{s=2}^{i} \chi_s \right) + \xi_i u_i u_{i+1}. \tag{48}$$

Step n: Select the Barrier Lyapunov function candidate

$$\mathcal{V}_{Ln} = \mathcal{V}_{L(n-1)} + \frac{1}{2} \log \frac{1}{1-u_n^2} + \frac{1}{2\gamma_{n1}} \tilde{\theta}_n^\top \tilde{\theta}_n + \frac{1}{2\gamma_{n2}} \tilde{\chi}_n^2, \tag{49}$$

where $\tilde{\theta}_n = \theta - \hat{\theta}_n$, $\tilde{\chi}_n = \chi_n - \hat{\chi}_n$, and γ_{n1}, γ_{n2} are positive values. Using the definition of u_n, we obtain $\dot{u}_n = \dot{\zeta}_n e_n + \zeta_n [u + (\varphi_n^\top - \sum_{s=1}^{n-1} \frac{\partial \alpha_{n-1}}{\partial x_s} \varphi_s^\top) \theta - \Delta_n + \Psi_n]$ where Δ_n and Ψ_n can be obtained from Δ_i and Ψ_i (let $i = n$).

Invoking (2), it can be deduced as

$$\begin{aligned} \dot{\mathcal{V}}_{Ln} \leqslant & -\ell(w) - \sum_{s=1}^{n-1} [c_s u_s^2 + \kappa_1 (\tilde{\theta}_s^\top \hat{\theta}_s + \tilde{\chi}_s \hat{\chi}_s)] + \kappa_1 \left(\frac{\chi_1}{d_s} + \sum_{s=2}^{i} \chi_s \right) + \xi_n \dot{\zeta}_n u_n e_n \\ & + \xi_{n-1} u_{n-1} u_n + \xi_n \zeta_n u_n \left[\rho u_f(t) + u_s - \Delta_n + \Psi_n + \left(\varphi_n - \sum_{s=1}^{n-1} \frac{\partial \alpha_{n-1}}{\partial x_s} \varphi_s \right)^\top \theta \right] \\ & - \frac{1}{\gamma_{n1}} \tilde{\theta}_n^\top \dot{\hat{\theta}}_n - \frac{1}{\gamma_{n2}} \tilde{\chi}_n \dot{\hat{\chi}}_n. \end{aligned} \tag{50}$$

Similar to step i, one has $\xi_n \zeta_n u_n \Psi_n \leqslant \chi_n \kappa_1 + \xi_n \zeta_n u_n \eta_n \chi_n$ with $\eta_n = [(\xi_n \zeta_n u_n \psi_n^\top \psi_n)(\sqrt{\xi_n^2 \zeta_n^2 u_n^2 \psi_n^\top \psi_n + \kappa_1^2})]$. By using Assumption 2, we have $\xi_n \zeta_n u_n u_s \leqslant |\xi_n \zeta_n u_n| \varpi$. Besides, to handle the actuator failure, we define $\mu = \frac{1}{\underline{\rho}}$ and $\hat{\mu} = \mu - \tilde{\mu}$. We introduce the following intermediate variable:

$$\begin{aligned} \beta = & \frac{\xi_n \zeta_n u_n \hat{\varpi}^2}{\sqrt{\xi_n^2 \zeta_n^2 u_n^2 \hat{\varpi}^2 + \kappa_1^2}} + \frac{\xi_{n-1} u_{n-1}}{\xi_n \zeta_n} + \frac{c_n u_n}{\xi_n \zeta_n} + \frac{\dot{\zeta}_n e_n}{\zeta_n} \\ & + \hat{\theta}_n^\top \left(\varphi_n - \sum_{s=1}^{n-1} \frac{\partial \alpha_{n-1}}{\partial x_s} \varphi_s \right) - \Delta_n + \hat{\chi}_n \eta_n + \frac{\xi_n \zeta_n u_n}{2(1-\varsigma_1)}, \end{aligned} \tag{51}$$

where c_n is a positive value, $0 < \varsigma_1 < 1$, and $\hat{\varpi} = \varpi - \tilde{\varpi}$.

Substituting β into (50) and by mathematical calculation yields that

$$\begin{aligned}\dot{\mathcal{V}}_{Ln} \leqslant &- \ell(w) - \sum_{s=1}^{n-1}[c_s u_s^2 + \kappa_1(\tilde{\theta}_s^\top \hat{\theta}_s + \tilde{\chi}_s \hat{\chi}_s)] - c_n u_n^2 + \kappa_1\left(\frac{\chi_1}{d_s} + \sum_{s=2}^{n} \chi_s\right) \\ &+ \xi_n \zeta_n u_n \left[\rho u_f(t) + \beta + \tilde{\chi}_n \eta_n + \tilde{\theta}_n^\top \left(\varphi_n - \sum_{s=1}^{n-1} \frac{\partial \alpha_{n-1}}{\partial x_s}\varphi_s\right)\right] + |\xi_n \zeta_n u_n|\varpi \\ &- \frac{\xi_n^2 \zeta_n^2 u_n^2 \hat{\varpi}^2}{\sqrt{\xi_n^2 \zeta_n^2 u_n^2 \hat{\varpi}^2 + \kappa_1^2}} - \frac{\xi_n^2 \zeta_n^2 u_n^2}{2(1-\varsigma_1)} - \frac{1}{\gamma_{n1}}\tilde{\theta}_n^\top \dot{\hat{\theta}}_n - \frac{1}{\gamma_{n2}}\tilde{\chi}_n \dot{\hat{\chi}}_n.\end{aligned} \tag{52}$$

To conserve communication resources, design the following adaptive event-based fault-tolerant controller:

$$u_f(t) = u_e(t_p),\ \forall t \in [t_p, t_{p+1}), \tag{53}$$

$$u_e(t) = -(1+\varsigma_1)\left(\frac{\xi_n \zeta_n u_n u_*^2}{\sqrt{(\xi_n \zeta_n u_n u_*)^2 + \kappa_3^2}} - \frac{\xi_n \zeta_n u_n \check{\epsilon}^2}{\sqrt{(\xi_n \zeta_n u_n \check{\epsilon})^2 + \kappa_3^2}}\right), \tag{54}$$

$$u_* = -\frac{\xi_n \zeta_n u_n \beta^2 \hat{\mu}^2}{\sqrt{\xi_n^2 \zeta_n^2 u_n^2 \beta^2 \hat{\mu}^2 + \kappa_2^2}}, \tag{55}$$

where $0 < \varsigma_1 < 1$ and $\check{\epsilon} > \frac{\bar{\epsilon}}{1-\varsigma} > 0$ are design parameters. $\bar{\epsilon}$ is an upper bound of the function $\epsilon(t)$. κ_2, κ_3 and $\epsilon(t)$ are chosen as the positive integral functions the same as κ_1. The measurement error is indicated by $\phi(t) = u_e(t) - u_f(t)$. The update time of actuator is denoted by t_p, and $u_f(t)$ holds $u_f(t) = u_e(t_p),\ t \in [t_p, t_{p+1})$.

At this point, we devise the following dynamic event-triggered mechanism (DETM) that can significantly trade-off system performance

$$t_{p+1} = \inf\{t > t_p | |\phi(t)| - \varsigma_1 |u_f(t)| - \epsilon(t) \geqslant \digamma(t)\}, \tag{56}$$

$$\dot{\digamma}(t) = -\varsigma_2 \digamma(t) + (\varsigma_1 |u_f(t)| + \epsilon(t) - |\phi(t)|), \tag{57}$$

where $\varsigma_2 > 0$.

Note that from (56), it is easy to get that $|\phi(t)| - \varsigma_1 |u_f(t)| - \epsilon(t) \leqslant \digamma$. Then, it can be obtained from (57) that $\dot{\digamma} \geqslant -(\varsigma_2 - 1)\digamma$, which indicates that $\digamma \geqslant \digamma(0) e^{-(\varsigma_2 - 1)t} \geqslant 0$.

Remark 5. The developed dynamic triggering threshold approach outperforms conventional fixed and relative threshold strategies [29, 30, 36] in managing network constraints and maintaining system performance. If $\digamma = 0$, then the static triggering strategy can be obtained,

$$t_{p+1} = \inf\{t > t_p | |\phi(t)| - \varsigma_1 |u_f(t)| - \epsilon(t) \geqslant 0\}. \tag{58}$$

Compared with the static triggering strategy, the dynamic triggering threshold method has much flexibility in control signal transmission.

Proposition 1. Let $\Delta t_s = t_{p+1}^s - t_p^s$ and $\Delta t_d = t_{p+1}^d - t_p^d$ as the interevent intervals for the dynamic triggering condition (57) and the static triggered condition (58), respectively. Then, we can obtain $\Delta t_d \geqslant \Delta t_s$.

Proof. Using the contradiction method, assume that $\Delta t_d \leqslant \Delta t_s$ with $t_p^s = t_p^d$. At $t = t_{p+1}^d$, it can be derived that

$$t_{p+1}^s \leqslant t_{p+1}^d,\ |\phi(t)| - \varsigma_1 |u_f(t)| - \epsilon(t) < 0. \tag{59}$$

Based on the above inequality and (56), we can further get that

$$0 > |\phi(t)| - \varsigma_1 |u_f(t)| - \epsilon(t) \geqslant \digamma(t_{p+1}^d), \tag{60}$$

which contradicts the positivity of $\digamma(t)$. On the other hand, it can be get that $\Delta t_d \geqslant \Delta t_s$. Since $t_p^s = t_p^d$, the interevent time with the static triggering strategy is less than that with the dynamic triggering strategy. Hence, the Zeno behavior can be excluded.

The case is possible for time-varying functions $o_1(t)$ and $o_2(t)$ to fulfill the conditions $|o_1(t)|,\ |o_2(t)| \leqslant 1$ resulting in $u_e(t) = (1 + \varsigma o_1(t)) u_f(t) + o_2(t)\epsilon(t)$. Consequently, one obtains

$$u_f(t) = \frac{u_e(t) - o_2(t)(\epsilon(t) + \digamma(t))}{1 + \varsigma_1 o_1(t)}. \tag{61}$$

Note that $o_1(t)$ and $o_2(t)$ are used only for stability analysis and not for control design. Besides, one can obtain $u_n \frac{u_e(t)}{1+\varsigma_1 o_1(t)} \leqslant u_n \frac{u_e(t)}{1+\varsigma_1}$ and $-\frac{o_2(t)(\epsilon(t)+\digamma(t))}{1+\varsigma_1 o_1(t)} \leqslant \frac{\epsilon(t)+\digamma(t)}{1-\varsigma_1} \leqslant \frac{\bar{\epsilon}}{1-\varsigma_1} + \frac{\digamma(t)}{1-\varsigma_1}$, thus,

$$\begin{aligned}\xi_n\zeta_n u_n u_f(t) \leqslant & -\frac{\xi_n^2\zeta_n^2u_n^2u_*^2}{\sqrt{(\xi_n\zeta_n u_n u_*)^2+\kappa_3^2}} - \frac{\xi_n^2\zeta_n^2u_n^2\check{\epsilon}^2}{\sqrt{(\xi_n\zeta_n u_n\check{\epsilon})^2+\kappa_3^2}} + |\xi_n\zeta_n u_n\check{\epsilon}| + \frac{|\xi_n\zeta_n u_n|\rho\digamma(t)}{1-\varsigma_1} \\ \leqslant & -\frac{\xi_n^2\zeta_n^2u_n^2u_*^2}{\sqrt{(\xi_n\zeta_n u_n u_*)^2+\kappa_3^2}} + |\xi_n\zeta_n u_n u_*| + \xi_n\zeta_n u_n u_* + \kappa_3 + \frac{|\xi_n\zeta_n u_n|\rho\digamma(t)}{1-\varsigma_1} \\ \leqslant & 2\kappa_3 + \xi_n\zeta_n u_n u_* + \frac{|\xi_n\zeta_n u_n|\rho\digamma(t)}{1-\varsigma_1}.\end{aligned} \tag{62}$$

According to $0<\lambda<\frac{\min(\gamma T,\gamma m)}{2mL}$, the parameters λ, γ, δ_1, and δ_2 can be selected such that

$$\begin{cases} T-m\nu^2 \geqslant 0, \\ \tau_2 = \lambda T - \lambda m b_1^2 - 2\lambda c L\delta_2 > 0, \\ \tau_3 = \gamma c - \frac{2\lambda c L}{\delta_2} > 0, \\ \tau_5 = \lambda m L\nu^2 - \frac{\gamma T\nu}{2} + \frac{\gamma T\delta_1}{2} - \lambda T L \geqslant 0, \\ \tau_6 = \frac{\gamma T}{2\delta_1} - \lambda m L. \end{cases} \tag{63}$$

3.3 Stability analysis

In this part, stability analysis of the closed-loop systems is provided.

Theorem 1. Under Assumptions 1–3 and bounded initial conditions, assuming that there exists a nonzero positive lower bound on the inter-event times given by $t_{p+1}-t_p>0$, if parameters λ, γ, δ_1, δ_2 are properly chosen such that $\tau_i>0$ $(i=1,\ldots,6)$, with the designed adaptive event-based fault-tolerant controller (53) and adaptive control laws (30)–(32), (38)–(40), (45)–(47), and (70)–(72), then we can obtain the following:

(1) all the closed-loop signals $\hat{\theta}_i, \hat{\chi}_i, x_i, e_i$ $(i=1,\ldots,n)$, $\alpha_1,\ldots,\alpha_{n-1}$, $\hat{\mu}$, $\hat{\varpi}$, and u_e are uniformly bounded;

(2) vibration displacement converges to zero, i.e., $\lim_{t\to\infty}|w(z,t)|=0$;

(3) e_i can be steered into the prescribed precision set $\{e_i|\ |e_i|<\varepsilon_i\}$ for $t\geqslant T_{pi}$.

Proof. Select the following global Lyapunov function candidate:

$$\mathcal{V} = \mathcal{V}_{Ln} + \frac{\rho}{2\Gamma_1}\tilde{\mu}^2 + \frac{1}{2\Gamma_2}\tilde{\varpi}^2 + \frac{1}{2}\digamma^2, \tag{64}$$

where $\tilde{\mu}=\mu-\hat{\mu}$ and Γ_1 and Γ_2 are positive constants. Considering (52) and (62), one has

$$\begin{aligned}\dot{\mathcal{V}} \leqslant & -\ell(w) - \sum_{s=1}^{n-1}[c_s u_s^2 + \kappa_1(\tilde{\theta}_s^\top\hat{\theta}_s + \tilde{\chi}_s\hat{\chi}_s)] - c_n u_n^2 + \kappa_1\left(\frac{\chi_1}{d_s} + \sum_{s=2}^n \chi_s\right) - \frac{\xi_n^2\zeta_n^2u_n^2}{2(1-\varsigma_1)} \\ & - \frac{\xi_n^2\zeta_n^2u_n^2\hat{\varpi}^2}{\sqrt{\xi_n^2\zeta_n^2u_n^2\hat{\varpi}^2+\kappa_2^2}} + \xi_n\zeta_n u_n\left[\tilde{\theta}_n^\top\left(\varphi_n - \sum_{s=1}^{n-1}\frac{\partial\alpha_{n-1}}{\partial x_s}\varphi_s\right) + \rho u_* + \beta\right] + 2\kappa_3 + |\xi_n\zeta_n u_n|\varpi \\ & + \frac{|\xi_n\zeta_n u_n|\rho\digamma}{1-\varsigma_1} - \varsigma_2\digamma^2 - \digamma[|\phi(t)| - \varsigma_1|u_f(t)| - \epsilon(t)] - \frac{1}{\gamma_{n1}}\tilde{\theta}_n^\top\dot{\hat{\theta}}_n - \frac{1}{\gamma_{n2}}\tilde{\chi}_n\dot{\hat{\chi}}_n - \frac{\rho}{\Gamma_1}\tilde{\mu}\dot{\hat{\mu}} - \frac{1}{\Gamma_2}\tilde{\varpi}\dot{\hat{\varpi}}.\end{aligned} \tag{65}$$

From (53), we obtain

$$\xi_n\zeta_n u_n\rho u_* \leqslant -\frac{\underline{\rho}\xi_n^2\zeta_n^2u_n^2\beta^2\hat{\mu}^2}{\sqrt{\xi_n^2\zeta_n^2u_n^2\beta^2\hat{\mu}^2+\kappa_2^2}} \leqslant -\underline{\rho}\xi_n\zeta_n u_n\beta\hat{\mu} + \underline{\rho}\kappa_2, \tag{66}$$

$$|\xi_n\zeta_n u_n|\varpi - \frac{\xi_n^2\zeta_n^2u_n^2\hat{\varpi}^2}{\sqrt{\xi_n^2\zeta_n^2u_n^2\hat{\varpi}^2+\kappa_1^2}} \leqslant |\xi_n\zeta_n u_n|\tilde{\varpi} + \kappa_1. \tag{67}$$

Meanwhile, using the Young's inequality, it can be obtained that

$$\frac{|\xi_n\zeta_n u_n|\rho\digamma}{1-\varsigma_1} \leqslant \frac{\xi_n^2\zeta_n^2u_n^2}{2(1-\varsigma_1)} + \frac{\digamma^2}{2(1-\varsigma_1)}. \tag{68}$$

Design the piecewise updating law

$$\begin{aligned}\dot{\hat{\mu}} &= \mathrm{proj}_{[1,1/\underline{\rho}]}\{\mathcal{K}\} \\ &= \begin{cases} 0, & \hat{\mu}=1 \text{ and } \mathcal{K}\leqslant 0 \text{ or } \hat{\mu}=1/\underline{\rho} \text{ and } \mathcal{K}\geqslant 0, \\ \mathcal{K}, & \text{otherwise}\end{cases}\end{aligned} \tag{69}$$

with $\mathcal{K}=\begin{cases}\Gamma_1\xi_n\zeta_n u_n\beta, & \text{if } \mathcal{M}\geqslant 0,\\ 0, & \text{if } \mathcal{M}\leqslant 0,\end{cases}$ and $\mathcal{M}=\Gamma_1\xi_n\zeta_n u_n\beta$. $\mathrm{proj}\{\cdot\}$ denotes the projection operator which restricts $\hat{\mu}$ to the interval $[1,1/\underline{\rho}]$. Some specific information about projection operator can be found in [39].

Choose the following adaptive updating laws:

$$\dot{\hat{\theta}}_n = \gamma_n\xi_n\zeta_n u_n\left(\varphi_n-\sum_{s=1}^{n-1}\frac{\partial\alpha_{n-1}}{\partial x_s}\varphi_s\right)-\gamma_n\kappa_1\hat{\theta}_n, \tag{70}$$

$$\dot{\hat{\chi}}_n = \gamma_{n2}\xi_n\zeta_n u_n\eta_n-\gamma_{n2}\kappa_1\hat{\chi}_n, \tag{71}$$

$$\dot{\hat{\varpi}} = \Gamma_2|\xi_n\zeta_n u_n|-\Gamma_2\kappa_1\hat{\varpi}. \tag{72}$$

Substituting (69)–(72) into (65) and based on the designed dynamic triggered strategy (56), then it can be derived as

$$\begin{aligned}\dot{\mathcal{V}} \leqslant & -\ell(w)-\sum_{s=1}^{n}[c_s u_s^2+\kappa_1(\tilde{\theta}_s^\top\hat{\theta}_s+\tilde{\chi}_s\hat{\chi}_s)]-\left(\varsigma_2-\frac{1}{2(1-\varsigma_1)}\right)F^2 \\ & +\kappa_1\left(\tilde{\varpi}\hat{\varpi}+\tilde{\mu}\hat{\mu}+\frac{\chi_1}{d_s}+\sum_{s=2}^{n}\chi_s+1\right)+\underline{\rho}\kappa_2+2\kappa_3.\end{aligned} \tag{73}$$

Using the complete square formula, we have $\tilde{\theta}_s^\top\hat{\theta}_s=-\tilde{\theta}_s^\top\tilde{\theta}_s+\tilde{\theta}_s^\top\theta_s\leqslant\frac{\theta_s^\top\theta_s}{4}$, $\tilde{\chi}_s\hat{\chi}_s=-\tilde{\chi}_s\tilde{\chi}_s+\tilde{\chi}_s\chi_s\leqslant\frac{\chi_s^2}{4}$, $\tilde{\varpi}\hat{\varpi}=-\tilde{\varpi}\tilde{\varpi}+\tilde{\varpi}\varpi\leqslant\frac{\varpi^2}{4}$, and $\tilde{\mu}\hat{\mu}=-\tilde{\mu}\tilde{\mu}+\tilde{\mu}\mu\leqslant\frac{\mu^2}{4}$. Then we arrive at

$$\dot{\mathcal{V}}\leqslant-\ell(w)-\sum_{s=1}^{n}c_s u_s^2-\left(\varsigma_2-\frac{1}{2(1-\varsigma_1)}\right)F^2+\sum_{s=1}^{3}\kappa_s\mathcal{C}_s, \tag{74}$$

where $\mathcal{C}_1=\sum_{s=1}^{n}(\frac{\theta_s^\top\theta_s}{4}+\frac{\chi_s^2}{4})+\frac{\mu^2}{4}+\frac{\chi_1}{d_s}+\sum_{s=2}^{n}\chi_s+\frac{\varpi^2}{4}+1$, $\mathcal{C}_2=\underline{\rho}$, and $\mathcal{C}_3=2$.

Using the definition of $\ell(w)$ and integrating it from 0 to t, i.e.,

$$\begin{aligned}\mathcal{V}(t)\leqslant & \mathcal{V}(0)-\int_0^t\int_0^L\left(\tau_1 w_t^2+\tau_2 w_z^2+\tau_3(w_t+\nu w_z)^2\right)dzdt \\ & -\int_0^t\left(\tau_4 w_z^2(0,t)+\tau_5 w_z^2(L,t)+\tau_6 w_t^2(L,t)\right)dt-\sum_{s=1}^{n}c_s\int_0^t u_s^2(t)dt \\ & -\left(\varsigma_2-\frac{1}{2(1-\varsigma_1)}\right)\int_0^t F^2(t)dt+\sum_{s=1}^{3}\mathcal{C}_s\int_0^t\kappa_s(t)dt.\end{aligned} \tag{75}$$

Since τ_i $(i=1,\ldots,6)$ and c_s are positive, we can obtain $\mathcal{V}(t)\leqslant\mathcal{V}(0)+\Upsilon$ with $\Upsilon=\sum_{s=1}^{3}\mathcal{C}_s\bar{\kappa}_s$, indicating that $\log\frac{1}{1-u_i^2},\tilde{\theta}_i,\tilde{\chi}_i,\tilde{\mu}$ and $\tilde{\varpi}$ are bounded. From the definition of $\tilde{\theta}_i,\tilde{\chi}_i,\tilde{\mu},\tilde{\varpi}$, then $\hat{\theta}_i,\hat{\chi}_i,\hat{\mu},\hat{\varpi}$ are uniformly bounded. As $\int_0^L w_z^2dz$ is bounded, from Poincaré's inequality $w(z,t)$ is bounded. Since $u_i(0)=\zeta_i(0)|e_i(0)|<1$ holds, it is concluded that $u_i(t)$ always remains within the set $\Omega_{u_i}=\{u_i(t)\in\mathbb{R}||u_i(t)|<1\}$, and thus $\xi_i(t)$ is bounded. Based on the definition of $\zeta_i(t)$, $\zeta_i(t)$ is bounded for $t>0$ and $\zeta_i(t)=0$ when $t=0$. As $e_i(0)$ is bounded, and thus $e_i(t)=u_i(t)/\zeta_i(t)$ holds and is bounded. Under Property 1, this leads to the boundedness of x_1 based on Assumptions 1 and 3. Note that α_1 is also a smooth function of bounded signals x_1, $w_t(L)$, $w_z(L)$, ζ_1, $\dot{\zeta}_1$, $\hat{\theta}_1$ and $\hat{\chi}_1$. It is concluded that α_1 is bounded. This also gives the boundedness of x_2 based on Assumptions 1 and 3. α_{i-1} is a smooth function of bounded signals $x_1,\ldots,x_{i-1}$, $w_t(L)$, $w_z(L)$, ζ_1, $\dot{\zeta}_1,\ldots,\zeta_{i-1}$, $\dot{\zeta}_{i-1}$, $\hat{\theta}_1,\ldots,\hat{\theta}_{i-1}$, $\hat{\chi}_1,\ldots,\hat{\chi}_{i-1}$. This also gives the boundedness of x_{i-1}. Likewise, the boundedness of u_e can also be obtained. Thus, we can conclude that all the closed-loop signals are bounded.

The inequality (75) indicates that $\int_0^L w_z^2 dz \in \mathcal{L}_\infty$. When $t \to \infty$, we further obtain $\lim_{t\to\infty} \int_0^t \int_0^L w_z^2 dz dt$ is bounded, that is, $\int_0^L w_z^2 dz \in \mathcal{L}_2$. Using Barbalat's Lemma, it can be obtained $\lim_{t\to\infty} \int_0^L w_z^2 dz = 0$. It follows from Poincaré's inequality that $\lim_{t\to\infty} |w(z,t)| = 0$, i.e., the asymptotic vibration suppression is achieved. It is known that $u_i(t)$ always remains within Ω_{u_i}, i.e., the variable $e_i(t)$ always evolves within the prescribed-time performance funnel (8). Using the third property of $\zeta_i(t)$, we can derive that $|e_i(t)| < \frac{1}{\zeta_i(t)} \leqslant \varepsilon_i$, $\forall t \geqslant T_{pi}$. Thus, the variable $e_i(t)$ can be steered into the prescribed region $(-\varepsilon_i, \varepsilon_i)$ within the preset time T_{pi}. The proof is completed.

Remark 6. Compared with [23–25] where the failure compensation problems were not addressed, this paper further considers the adaptive boundary failure compensation control for cascaded systems. When the failures occur, the control input $u(t)$ decreases, and the expected control performance cannot be obtained. To address this issue, an adaptive compensation coefficient $\hat{\mu}$ with adaptive mechanism (69) is introduced in this paper.

Remark 7. Unlike the existing studies, this paper has some distinctive characteristics: (1) the cascaded ODE-belt systems are allowed to have arbitrary relative degree and unmatched uncertainties, in contrast to the pure axially moving systems [1–7] and axially moving systems with first-order linear actuator dynamics [8–14]; (2) the limitation that the settling time is dependent on the initial conditions and design parameters is removed, unlike [20, 21]; (3) a new dynamic event-based fault-tolerant control is developed where the effects of actuator failures can be adaptively eliminated, contrary to [22–25]; (4) the proposed fault-tolerant controller can ensure asymptotic vibration suppression instead of the UUB results [1–6].

Remark 8. The parameters c_i, κ_1, κ_2, and κ_3 must be carefully adjusted to balance state convergence speed and control smoothness. Larger values of c_i achieve faster stabilization convergence but also result in a larger input signal and increase actuator burden. Additionally smaller values of κ_2 and κ_3 achieve faster convergence, but if they are too small, they may cause chattering owing to the control discontinuity. Hence, the trade-off between control performance and control effort should be adjusted according to the practical requirements.

4 Simulation results

This section validates the proposed adaptive event-based boundary fault-tolerant control protocol. We verify the proposed theoretical results through the application of the finite difference method [40–42] with time step $dt = 0.0001$ and space step $dz = 0.0204$.

Consider the actuator dynamics as a simplified Josephson circuit [15], i.e.,

$$\ddot{X} + \pi_1 \dot{X} + \pi_2 \sin(X) = u(t), \tag{76}$$

where π_1, π_2 are known parameters. If $x_1 = X$, $x_2 = \dot{X} + \pi_1 X$, the actuator dynamics can be expressed as $\dot{x}_1 = x_2 - \pi_1 x_1, \dot{x}_2 = u(t) - \pi_2 \sin(x_1)$. Letting $\theta = [\pi_1 \ \pi_2]$, $\varphi_1 = [-x_1 \ 0]$, and $\varphi_2 = [0 \ -\sin(x_1)]$, the actuator dynamics can be transformed into $\dot{x}_1 = x_2 + \varphi_1^\top \theta$, $\dot{x}_2 = u(t) + \varphi_2^\top \theta$. The unknown function $\Psi_1 = -m_c w_{tt}(L) - T w_z(L)$ will be approximated by using RBFNNs.

The system parameters for (1a)–(1g) are chosen as $m = 0.1$ kg/m, $T = 2000$ N, $c = 0.1$ Ns/m^2, $d_s = 0.8$ Ns/m, $m_c = 23$ kg, $L = 1$ m, $g = 9.8$ N/kg, $\kappa_a = \kappa_d = 3$ g, and $[r_1, r_2, r_3, r_4, r_5, r_6, r_7] = [1, 2, 3, 7, 8, 9, 10]$ s. The initial values of $w(z, 0)$, x_1, x_2, ν_0, $\hat{\mu}$, $\hat{\varpi}$, $\hat{\theta}_1$, $\hat{\theta}_2$, $\hat{\chi}_1$, and $\hat{\chi}_2$ are chosen as $w(z, 0) = 0.001 \sin(z)$, $x_1(0) = 0.2$, $x_2(0) = 0.1$, $\nu_0 = 0$ m/s, $\hat{\mu}(0) = 1$, $\hat{\chi}_1(0) = \hat{\chi}_2(0) = \hat{\varpi}(0) = 5$, $\hat{\theta}_1(0) = [8.9 \ 7.5]^\top$, $\hat{\theta}_2(0) = [5.5 \ 5.4]^\top$, and $F(0) = 0.5$. In this paper, the actuator u loses 50% of its effectiveness from $t = 3$ s and is subject to bias fault $u_s(t) = 0.12 \sin(5t)$.

Based on the aforementioned control design, the design parameters are chosen as $c_1 = 10.3$, $c_2 = 10$, $\gamma = 0.5$, $\delta_1 = \epsilon = 0.05$, $T_{p1} = T_{p2} = 5$, $q_1 = 4$, $q_2 = 3$, $\varepsilon_1 = 0.1$, $\varepsilon_2 = 0.9$, $\gamma_{11} = \gamma_{21} = 0.08$, $\gamma_{12} = \gamma_{22} = 1.5$, $\Gamma_1 = 0.03$, $\Gamma_2 = 0.1$, and $\kappa_1 = 100e^{-0.01t}$, $\varsigma_1 = 0.5$, $\varsigma_2 = 8.5$, $\kappa_2 = \kappa_3 = 400e^{-0.001t}$, $\epsilon(t) = 5e^{-0.001t}$, and $\check{\epsilon} = 5.8$.

The considered cascaded ODE-belt systems are simulated with the following cases for comparative analysis.

Case 1: Without control, i.e., $u(t) = 0$.

Case 2: With the proposed adaptive event-based boundary fault-tolerant control (53)–(55).

Case 3: With the Nussbaum function method in [26].

Case 4: With the static event-triggered mechanism (STEM) in [31].

To show the performance comparison, we introduce the following performance metrics: steady-state root-mean-square error ERMS $= \sqrt{\frac{1}{6}\int_4^{10}\int_0^1 w^2(z,t) dz dt}$, integral of steady-state absolute error IAE $= \int_4^{10}\int_0^1 |w(z,t)| dz dt$, and integral of steady-state time-weighted absolute error ITAE $= \int_4^{10}\int_0^1 t|w(z,t)| dz dt$. From Table 1, the advantages of the proposed event-based boundary fault-tolerant control strategy have been demonstrated.

Table 1 Performance metric and triggering method/number.

Case	ERMS	IAE	ITAE	Triggering
Case 1	0.000129	0.000493	0.002961	0
Case 2	0.000009	0.000020	0.000119	DETM/688
Case 3	0.000031	0.000119	0.000711	Time-triggered/100000
Case 4	0.000009	0.000024	0.000146	STEM/1042

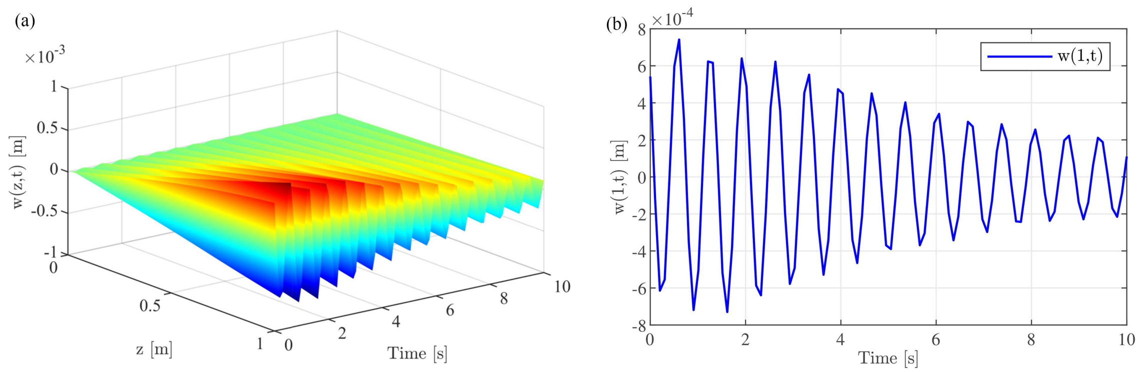

Figure 3 (Color online) (a) Vibration displacement $w(z,t)$ and (b) vibration deflection $w(1,t)$ in Case 1.

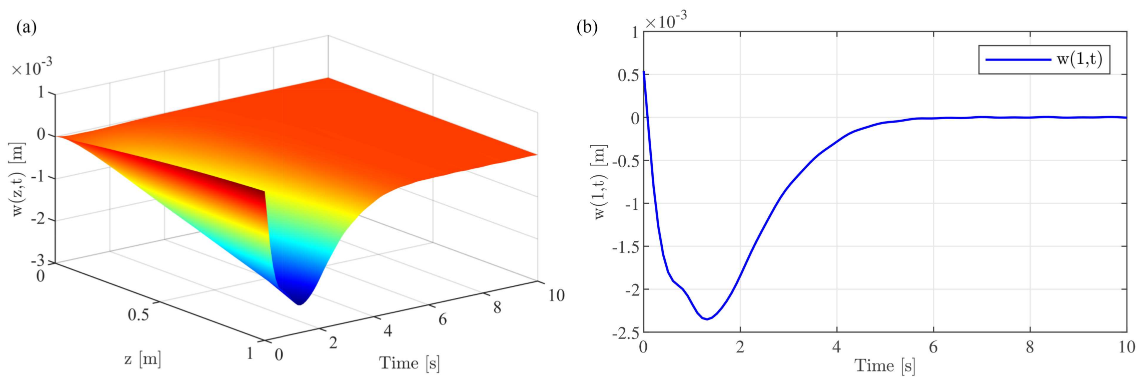

Figure 4 (Color online) (a) Vibration displacement $w(z,t)$ and (b) vibration deflection $w(1,t)$ in Case 2.

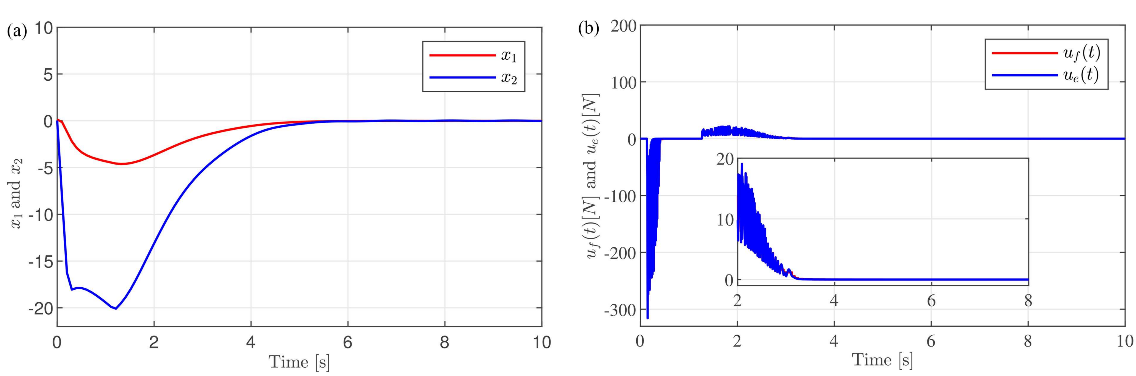

Figure 5 (Color online) (a) Actuator states x_1 and x_2 and (b) control input $u(t)$ in Case 2.

The simulation results for Cases 1–4 are provided in Figures 3–13. Figure 3 illustrates the vibration displacement $w(z,t)$ and deflection $w(1,t)$ for Case 1, in which the boundary vibration of the axially moving belt is very pronounced and disturbs the system performance and results in a deterioration of the control quality. Under the proposed adaptive event-based boundary fault-tolerant control (53)–(55), Figure 4 presents the vibration displacement $w(z,t)$ and the deflection $w(1,t)$ can be effectively suppressed. Under the Nussbaum function method in [27], it can be observed from Figure 9 that the vibration can be suppressed to some extent. Figures 5(a), 10(a), and

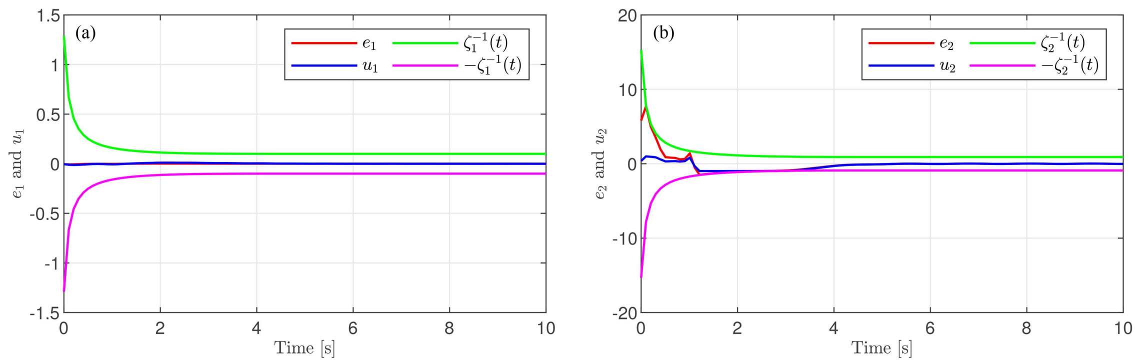

Figure 6 (Color online) Trajectories of (a) e_1 and u_1 and (b) e_2 and u_2 in Case 2.

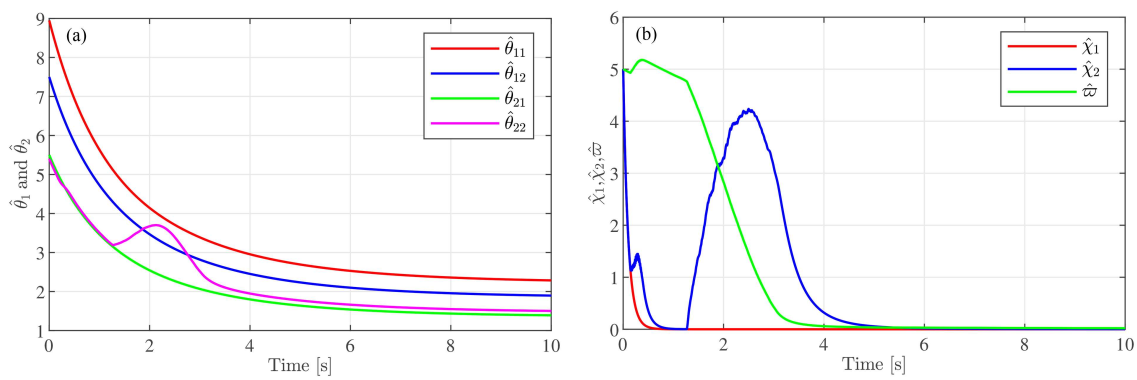

Figure 7 (Color online) Parameter estimation (a) $\hat{\theta}_1$ and $\hat{\theta}_2$ and (b) $\hat{\chi}_1$, $\hat{\chi}_2$, and $\hat{\varpi}$ in Case 2.

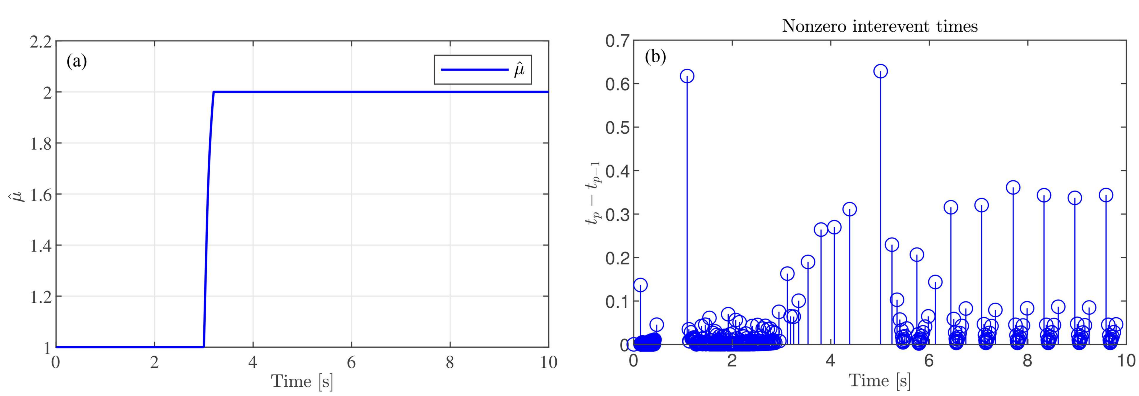

Figure 8 (Color online) (a) Parameter estimation $\hat{\mu}$ and (b) interevent time interval in Case 2.

13(a) show the actuator states $x_1(t)$ and $x_2(t)$ for Cases 2–4. Figures 5(b), 10(b), and 13(b) illustrate the evolutions of input signals $u_f(t)$ and $u_e(t)$. Overall, Figures 3, 4, 9, and 12 and Table 1 verify the effectiveness of the proposed adaptive event-based boundary fault-tolerant control (53)–(55) under actuator faults, unknown nonlinearities, and unknown parameters. Figures 6 and 11 illustrate the variables e_i and u_i and funnel functions, which indicate that the variable e_i converges within the prescribed set in the prescribed finite time $T_{pi} = 5$ for Cases 2 and 3. Besides, Figures 7 and 8(a) present the evolutions of adaptive parameter estimations $\hat{\theta}_1, \hat{\theta}_2, \hat{\varpi}, \hat{\chi}_1, \hat{\chi}_2$, and $\hat{\mu}$. Moreover, it can be seen that when an actuator fault occurs, the adaptive compensation variable $\hat{\mu}$ will increase to compensate for the effect of actuator fault. From Table 1, the triggering rate of the cascaded ODE-belt systems is $\frac{688}{100000} = 0.69\%$. This indicates that the proposed dynamic event-triggering strategy can avoid a large number of updates, thereby saving control resources. Additionally, Figure 8(b) presents the time interval in which the minimum interval remains strictly positive, verifying the exclusion of Zeno behavior.

Remark 9. Since $\lambda, m > 0$, we have $\tau_1 = \lambda m > 0$. The axial speed $\nu(t) \in [\nu_0, \nu_{\max}] = [0, 68.6]$ can be obtained in [3]. Then it is easy to get that $T - m\nu^2 \geqslant T - mb_1^2 = 1058.808 > 0$, and hence $\tau_4 = [\gamma\nu(T - m\nu^2)]/2 > 0$.

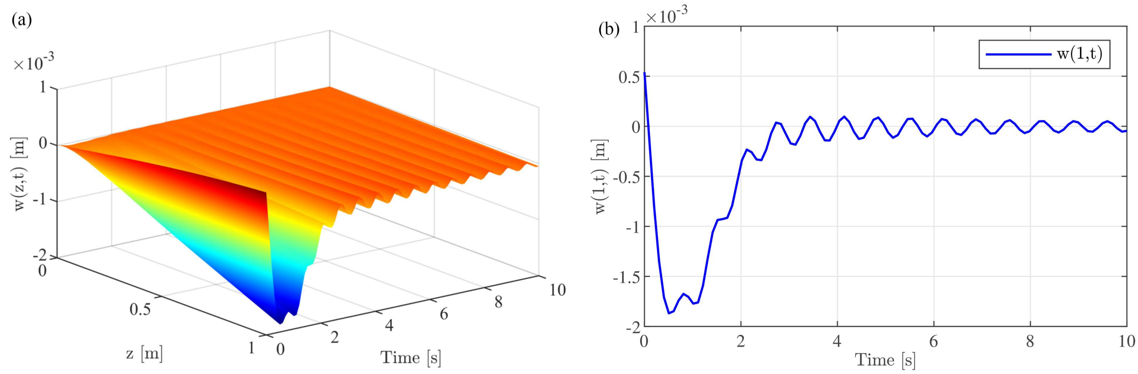

Figure 9 (Color online) (a) Vibration displacement $w(z,t)$ and (b) vibration deflection $w(1,t)$ in Case 3.

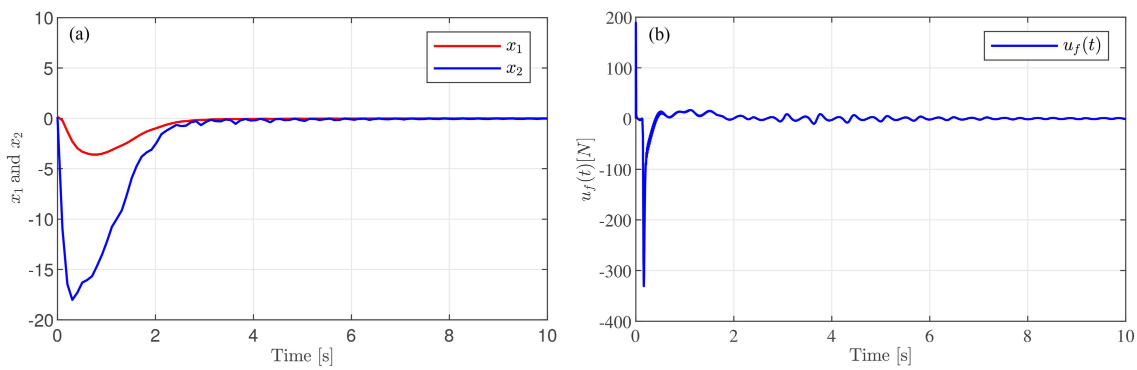

Figure 10 (Color online) (a) Actuator states x_1 and x_2 and (b) control input $u(t)$ in Case 3.

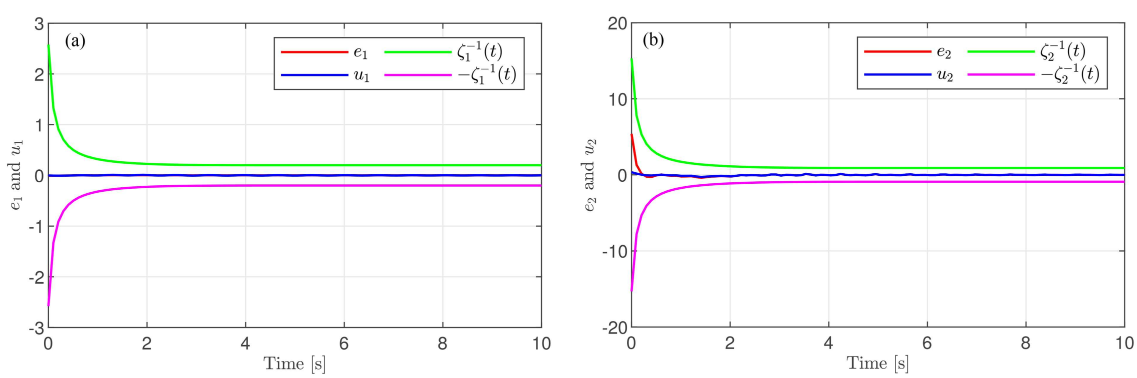

Figure 11 (Color online) Trajectories of (a) e_1 and u_1 and (b) e_2 and u_2 in Case 3.

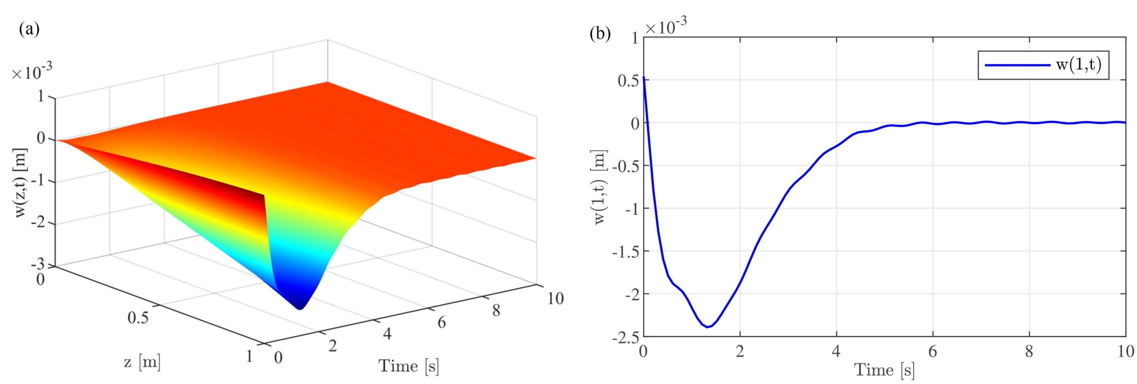

Figure 12 (Color online) (a) Vibration displacement $w(z,t)$ and (b) vibration deflection $w(1,t)$ in Case 4.

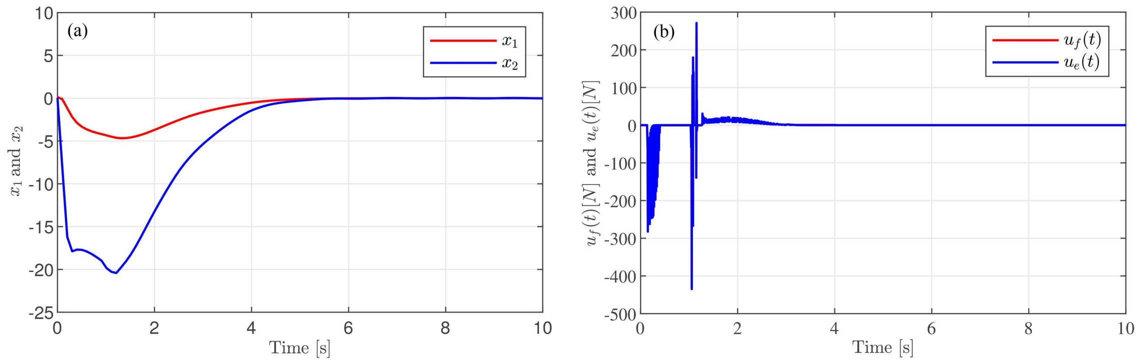

Figure 13 (Color online) (a) Actuator states x_1 and x_2 and (b) control input $u(t)$ in Case 4.

Through mathematical calculations, one has $\tau_2 = \lambda T - \lambda m b_1^2 - 2\lambda c L \delta_2 = 1.527 > 0$, $\tau_3 = \gamma c - \frac{2\lambda c L}{\delta_2} = 0.001 > 0$, and $\tau_6 = \frac{\gamma T}{2\delta_1} - \lambda m L = 0.143 > 0$. Letting $F = \lambda m L \nu^2 - \frac{\gamma T \nu}{2} + \frac{\gamma T \delta_1}{4} - \lambda T L$, we can obtain $F = 0.0001\nu^2 - 10\nu + 698$ with $\nu \in [0, 68.6]$. The solutions s_1, s_2 of $F = 0$ can be obtained as $s_1 = 69.849$ and $s_2 = 99932.151$, which indicates that F is a monotone decreasing function when $\nu \in [0, 68.6]$. Hence, substituting $\nu_{\max}$ into F, we can get $\lambda L \nu^2 - \frac{\gamma T \nu}{2} + \frac{\gamma T k_1}{4} - \lambda T L = 14.471 > 0$, i.e., $\tau_5 > 0$. Therefore, according to the above analysis, we can conclude that the conditions (63) can be satisfied by choosing appropriate values of $\lambda, \gamma, \delta_1, \delta_2$.

5 Conclusion

In this paper, we mainly investigate event-based boundary control of cascaded ODE-belt systems with nonlinearities, unknown parameters, actuator fault, and prescribed-time performance. In this case, it is a challenging task to realize the asymptotic stabilization of cascaded ODE-belt systems. Based on the prescribed-time performance funnel functions, combined with the BLF method and bounded estimation method, a new event-based boundary control algorithm is presented. Besides, a new failure compensator is proposed to adaptively eliminate the effect of actuator failure. Under the proposed control protocol and Barbalat's Lemma, asymptotic stabilization control of cascaded ODE-belt systems can be achieved. Finally, numerical simulation results well demonstrate the advantages of the designed control algorithm. In future work, we will focus on the boundary active fault-tolerant control of flexible axially moving system with unknown direction fault and monotonic tube performance boundaries.

Acknowledgements This work was supported in part by National Natural Science Foundation of China (Grant Nos. 62433011, 62503180, U25A20461), China Postdoctoral Science Foundation (CPSF) (Grant No. 2025M771726), Postdoctoral Fellowship Program of CPSF (Grant No. GZC20251196), National Key Laboratory of Space Intelligent Control (Grant No. HTKJ2025KL502026), China Scholarship Council (Grant No. 202506150127), and National Research Foundation of Korea (NRF) Grant funded by the Korean Government (MSIT) (Grant No. RS-2023-00208078).

References

1 He W, Ge S S, Zhang S. Adaptive boundary control of a flexible marine installation system. Automatica, 2011, 47: 2728–2734
2 Endo T, Matsuno F, Jia Y. Boundary cooperative control by flexible Timoshenko arms. Automatica, 2017, 81: 377–389
3 Zheng Y, Yao X, Liu Y. Event-triggered vibration control of an axially moving belt system with output constraint. IEEE Trans Syst Man Cybern Syst, 2025, 55: 4854–4863
4 Liu Y, Yao X, Zhao W. Distributed neural-based fault-tolerant control of multiple flexible manipulators with input saturations. Automatica, 2023, 156: 111202
5 Mohsenipour R, Liu G. Flexible single-link manipulators control based on a full-order transfer function model. IEEE Trans Automat Contr, 2024, 69: 4086–4093
6 Liu Y, Fu Y, He W, et al. Modeling and observer-based vibration control of a flexible spacecraft with external disturbances. IEEE Trans Ind Electron, 2018, 66: 8648–8658
7 Liu Z, Han Z, Zhao Z, et al. Modeling and adaptive control for a spatial flexible spacecraft with unknown actuator failures. Sci China Inf Sci, 2021, 64: 152208
8 Wang J, Krstic M. Output feedback boundary control of a heat PDE sandwiched between two ODEs. IEEE Trans Automat Contr, 2019, 64: 4653–4660
9 Krstic M, Bhan L, Shi Y. Neural operators of backstepping controller and observer gain functions for reaction C diffusion PDEs. Automatica, 2024, 164: 111649
10 Liu W J, Krstić M. Backstepping boundary control of Burgers' equation with actuator dynamics. Syst Control Lett, 2000, 41: 291–303

11 Meng T, Zhang Y, Fu Q, et al. Observer-based adaptive control for a coupled PDE-ODE system of a flexible wing. IEEE Trans Syst Man Cybern Syst, 2024, 54: 3949–3959
12 Zhao D, Jiang B, Yang H. Backstepping-based decentralized fault-tolerant control of hypersonic vehicles in PDE-ODE form. IEEE Trans Automat Contr, 2021, 67: 1210–1225
13 Liu Z, Liu J, He W. Robust adaptive fault tolerant control for a linear cascaded ODE-beam system. Automatica, 2018, 98: 42–50
14 Xing X, Liu J. Robust adaptive control allocation for a class of cascade ODE-string systems with actuator failures. IEEE Trans Automat Contr, 2021, 67: 1474–1481
15 Li J, Wu Z, Wen C. Adaptive stabilization for a reaction-diffusion equation with uncertain nonlinear actuator dynamics. Automatica, 2021, 128: 109594
16 Xiao Y, Yuan Y, Yang C, et al. Adaptive neural tracking control of a class of hyperbolic PDE with uncertain actuator dynamics. IEEE Trans Cybern, 2024, 54: 693–705
17 Liu Y, Chen X, Mei Y, et al. Observer-based boundary control for an asymmetric output-constrained flexible robotic manipulator. Sci China Inf Sci, 2022, 65: 139203
18 Tee K P, Ge S S, Tay E H. Barrier Lyapunov functions for the control of output-constrained nonlinear systems. Automatica, 2009, 45: 918–927
19 Liu L, Liu Y J, Chen A, et al. Integral barrier Lyapunov function-based adaptive control for switched nonlinear systems. Sci China Inf Sci, 2020, 63: 132203
20 Berger T. Input-constrained funnel control of nonlinear systems. IEEE Trans Automat Contr, 2024, 69: 5368–5382
21 Song Y D, Zhou S. Tracking control of uncertain nonlinear systems with deferred asymmetric time-varying full state constraints. Automatica, 2018, 98: 314–322
22 Boskovic J D, Mehra R K. Stable multiple model adaptive flight control for accommodation of a large class of control effector failures. In: Proceedings of the 1999 American Control Conference, 1999. 1920–1924
23 Wang W, Wen C. Adaptive actuator failure compensation control of uncertain nonlinear systems with guaranteed transient performance. Automatica, 2010, 46: 2082–2091
24 Zhang J X, Yang G H. Prescribed performance fault-tolerant control of uncertain nonlinear systems with unknown control directions. IEEE Trans Automat Contr, 2017, 62: 6529–6535
25 Zhai D, An L, Dong J, et al. Output feedback adaptive sensor failure compensation for a class of parametric strict feedback systems. Automatica, 2018, 97: 48–57
26 Cheng S, Wang Q G, Yu J, et al. Nussbaum-based fixed-time adaptive fault-tolerant control and its application to robot manipulator. IEEE Trans Consumer Electron, 2026, 72: 805–813
27 Guo X, Wang C, Liu L. Adaptive fault-tolerant control for a class of nonlinear multi-agent systems with multiple unknown time-varying control directions. Automatica, 2024, 167: 111802
28 Han Z, Liu Z, Wang J W, et al. Fault-tolerant control for flexible structures with partial output constraint. IEEE Trans Automat Contr, 2023, 69: 2668–2675
29 Xing L, Wen C, Liu Z, et al. Event-triggered adaptive control for a class of uncertain nonlinear systems. IEEE Trans Automat Contr, 2016, 62: 2071–2076
30 Zheng Y, Li Y X. Event-triggered output feedback consensus tracking control for nonlinear multiagent systems with sensor failures. Automatica, 2023, 148: 110787
31 Xing L, Wen C. Dynamic event-triggered adaptive control for a class of uncertain nonlinear systems. Automatica, 2023, 158: 111286
32 Chen Z, Han Q L, Yan Y, et al. How often should one update control and estimation: review of networked triggering techniques. Sci China Inf Sci, 2020, 63: 150201
33 Li Y, Li Y X, Tong S. Event-based finite-time control for nonlinear multiagent systems with asymptotic tracking. IEEE Trans Automat Contr, 2023, 68: 3790–3797
34 Rathnayake B, Diagne M, Espitia N, et al. Observer-based event-triggered boundary control of a class of reaction-diffusion PDEs. IEEE Trans Automat Contr, 2021, 67: 2905–2917
35 Wang J, Krstic M. Event-triggered output-feedback backstepping control of sandwich hyperbolic PDE systems. IEEE Trans Automat Contr, 2021, 67: 220–235
36 Liu Y J, Xu F, Tang L. Tangent barrier Lyapunov function based adaptive event-triggered control for uncertain flexible beam systems. Automatica, 2023, 152: 110976
37 Li W, Zhang H, Zhang J, et al. Fully distributed dynamic event-triggered formation-containment tracking for multiagent systems with multiple types of disturbances. Sci China Inf Sci, 2024, 67: 112203
38 De Queiroz M S, Dawson D M, Nagarkatti S P, et al. Lyapunov-Based Control of Mechanical Systems. Boston: Birkhauser, 2000. 213
39 Ioannou P A, Sun J. Robust Adaptive Control. Upper Saddle River: PTR Prentice-Hall, 1996
40 Yao X, Li X, Liu Z, et al. Asymptotical fault-tolerant time-varying tracking control of networked mobile flexible manipulators under prescribed performances and DoS attacks. IEEE Trans Automat Contr, 2026, 71: 20–35
41 Yao X, Xu X, He W, et al. Asymptotical event-based input-output constrained boundary control of flexible manipulator agents under a signed digraph. Sci China Inf Sci, 2025, 68: 142201
42 Liu Y, Lin C, Yao X. Attitude consensus and vibration control of flexible spacecraft with input quantization and asymmetric time-varying output constraints. IEEE Trans Cybern, 2026, doi: 10.1109/TCYB.2026.3677036